Doctoral Dissertation

Unravelling the N-linked Glycan Structures of Selected Ustilaginomycete Yeasts and Prospects of Glycan Information on Diversity, Biology and Biotechnology

FLORES RONILO JOSE DANILA

July 2020

International Program of Frontier Biotechnology,
Division of Advanced Science and Biotechnology,
Graduate School of Engineering,
Osaka University

TABLE OF CONTENTS

LIST OF ABBREVIATIONS

NP-HPLC	Normal-Phase High Performance Liquid Chromatography
DEAE- HPLC	Diethylaminoethyl High Performance Liquid Chromatography
RP- HPLC	Reversed-Phase High Performance Liquid Chromatography
LC-MS/MS	Liquid Chromatography Mass Spectrometry Mass Spectrometry
PCR	Polymerase Chain Reaction
PA	2-amino pyridine
NBRC	National Bioresource Center
BLAST	Basic Local Alignment Search Tool
PTM	Post-translational modifications
ER	Endoplasmic reticulum
DNA	Deoxyribonucleic Acid
Dol-PP	Dolichol Pyrrophoshate
OST	Oligosaccharyltransferase
Glc	Glucose
Man	Mannose
GlcNAc	N-acteylglucosamine
rDNA	Recombinant DNA
MEXT	Ministry of Education, Culture, Sports, Science and Technology (Japan)
YMB	Yeast Extract Malt Extract Broth
YPD	Yeast Peptone Dextrose Broth
TFA	Trifluoroacetic acid
NITE	National Institute of Technology and Evaluation

Chapter 1

Introduction

The Yeasts

Yeasts are phylogenetically classified into two phyla, the Ascomycota and the Basidiomycota. The yeasts under Ascomycota are taxonomically grouped under subphylum Saccharomycotina and Taphrinomycotina (Tendersoo et al., 2018; Hibbett et al., 2007). Subphylum Saccharomycotina includes certain genera like *Saccharomyces* and *Candida* while subphylum Taphrinomycotina includes the fission yeast *Schizosaccharomyces*. On the other hand, the basidiomycetous yeasts are taxonomically grouped under the subphylum Ustilaginomycotina, Agaricomycotina and Pucciniomycotina (Tedersoo et al., 2018; Hibbett et al., 2007; Boekhout 1991; Bauer et al., 1997; Boekhout et al., 2011). These basidiomycetous yeasts are dimorphic which means that they have both the yeast stage and the mycelial stage in their life cycles. Some basidiomycetous yeasts are known as plant pathogens like smuts and rusts while others are animal pathogens such as the genera *Cryptococcus, Trichosporon and Malassezia.* In addition, some basidiomycetous yeasts like *Pseudozyma, Sympodiomycopsis, Mrakia, Cystofilobasidium, Fellomyces, Filobasidium* and *Dioszegia* are either commensals of different plant species or are frequently isolated as part of the autochthonous populations in soil and other environments. Studies on yeast diversity and taxonomy have been very dynamic over the years leading to numerous new species being described and changes in the yeast taxonomy.

In this study, *Pseudozyma antarctica, Sympodiomycopsis paphiopedili* and *Malassezia. furfur*, belonging to the Ustilaginomycotina, were chosen as subjects of glycan structure analysis. *P. antarctica*, *S. paphiopedili* and *M. furfur* are species belonging to class Ustilaginomycetes, Exobasidiomycetes and Malasseziales, respectively (Tedersoo et al., 2018). *P. antarctica*, just like

any other species of *Pseudozyma*, is frequently isolated in plant material such as leaves flowers and stem (Boekhout and Fell, 1998). *S. paphiopedili* is the type species of the genus *Sympodiomycopsis* and was originally isolated from the nectar of the orchid *Paphiopedilum primurinum* in Japan (Sugiyama et al., 1991). In contrast to the two earlier species, *M. furfur* is naturally found on the skin surface of mammals and can become pathogenic due to some predisposing factors such as the health state of the host. Although there are several studies on these species about their biology, physiology ecology and biotechnological applications, their *N*-linked glycans have never been studied in the past except for *M. furfur* wherein galactofuranose-containing polysaccharides have been detected (Shibata et al., 2009). However, detailed information on the linkages of the galactofuranose residues to the *N*-linked glycans or whether it was linked to *N*-linked glycans has never been identified.

In juxtaposition, the Agaricomycotina contains roughly 20,000 described species, which is almost 70% of the known Basidiomycota and about 30% of all known fungal species (Hibbett et al., 2007; Hibett, 2006). About 98% of the species of the Agaricomycotina are in a class called the Agaricomycetes, which includes mushrooms, bracket fungi, puffballs, and others. The other major groups are the classes Tremellomycetes and Dacrymycetes. These latter groups include "jelly fungi", which have gelatinous, often translucent fruiting bodies (e.g. "witches` butter" *Tremella mesenterica*), as well as many yeast-forming species (Hibbett et al., 2007). Most of the members of Order Cystofilobasidiales (*Cystofilobasidium capitatum and Mrakia frigida*), Order Filobasidiales (*Fellomyces uniguttulatum*), Order Tremellales (*Dioszegia hungarica and Filobasidium polyborus*) and Order Trichosporonales (*Trichosporon cutaneum*) also have yeasts classified under Agaricomycotina. *M. frigida* and *C. capitatum* are both psychrophilic yeasts that

have been commonly isolated from a variety of cold environments such as marine sediments in Antarctica, soil, frozen fish and even snow. (Yamada and Komagata, 1987: Hua et al., 2010 and Nakagawa et al., 2002). It is said that these cold-adapted yeast species can be used in cold-fermentation and may produce some ezymes active in the cold environment (Hamid et al., 2014). *F. uniguttulatum* is commonly isolated from certain parts of the human body such as infected fingernail, white patches in mouth, bronchus and sole of the foot, and can become pathogenic like its close relative *Cryptococcus neoformans* causing meningitis (Pan et al., 2012). *Filobasidium neoformans* is a known teleomorph of *C. neoformans* (Guého et al., 1993). *D. hungarica* was determined to be a new species in 1957 and since then had undergone some revisions including when a certain genus of *Cryptococcus* has been emended as *D. hungarica* due to the advent of molecular data and polyphasic taxonomy. *Cryptococcus* is widely distributed in different environments such as soil and sediments and has had a number of new novel species assignments in the past decade (Takashima et al., 2001; Kirk et al., 2008; Takashima et al., 2011; Trochine et al., 2017; Connel et al., 2010). *F. polyborus* is also widely distributed in nature and is an anamorphic yeast species for the sterigma-containing Q10-equipped organisms. Hence, it was formerly named *Sterigmatomyces* (Yamada and Banno, 1984).
All species of *Trichosporon* are yeasts with no known teleomorphs. Most are typically isolated from soil, but several species such as *T. cutaneum* occur as a natural part of the skin microbiota of humans and other animals. Proliferation of the yeasts in hair can lead to an unpleasant but non-serious condition known as white piedra and may also cause a severe infection, trichosporonosis, in immunocompromised persons (Magalhaes et al., 2008; Middlehoven et al., 2004). On the other hand, subphylum Pucciniomycotina is another sister group of Ustilaginomycotina, Agaricomycotina and Wallemiomycotina (Tedersoo et al., 2018; Hibbett et al., 2007). The

subphylum Pucciniomycotina contains 10 classes and over 8400 species of Pucciniomycotina have been described which comprise more than 8% of all described fungi (Schell et al., 2011; Tendersoo et al., 2018). Fungi belonging to Pucciniomycotina are found in a diversity of habitats, including specialized niches that are historically undersampled for the Fungi. Ecologically, most of the discovered species are plant associates, predominantly phytopathogens but also include asymptomatic members of the phylloplane and species that form mycorrhizal associations with orchids (Aime et al., 2014). The taxonomic positions of the 3 ustilaginomycetous yeasts and the other mentioned yeasts are shown in Figure 1.

Proteins and Post-translational modification (PTM)

Glycans, a major class of carbohydrates found in majority of living organisms, play a significant role in disease development and have a wide range of functions which include protein folding and trafficking (Mitra et al., 2003). Protein glycosylation is one of the most abundant forms of post-translational modification, in which glycosylated proteins are found in nearly 50% of cellular proteins and 90% of secreted proteins (Agard and Bertozzi, 2009; Grobe et al., 2002). Cell wall proteins of microorganisms and protein coats of viruses are usually glycosylated and recognized in the human body as foreign molecules (Herrmann et al., 1997; Suzuki 2005; Upreti et al., 2003). Asparagine (*N*)-linked glycosylation, both present in eukaryotes and prokaryotes, is an extensive process that results in an oligosaccharide being bound to the asparagine (*N*)-residue of a polypeptide (Schwarz and Aebi, 2011). During early steps, *N*-linked glycosylation is conserved throughout the eukaryotic domain (Kukuruzinska and Lennon, 1998). However, in later

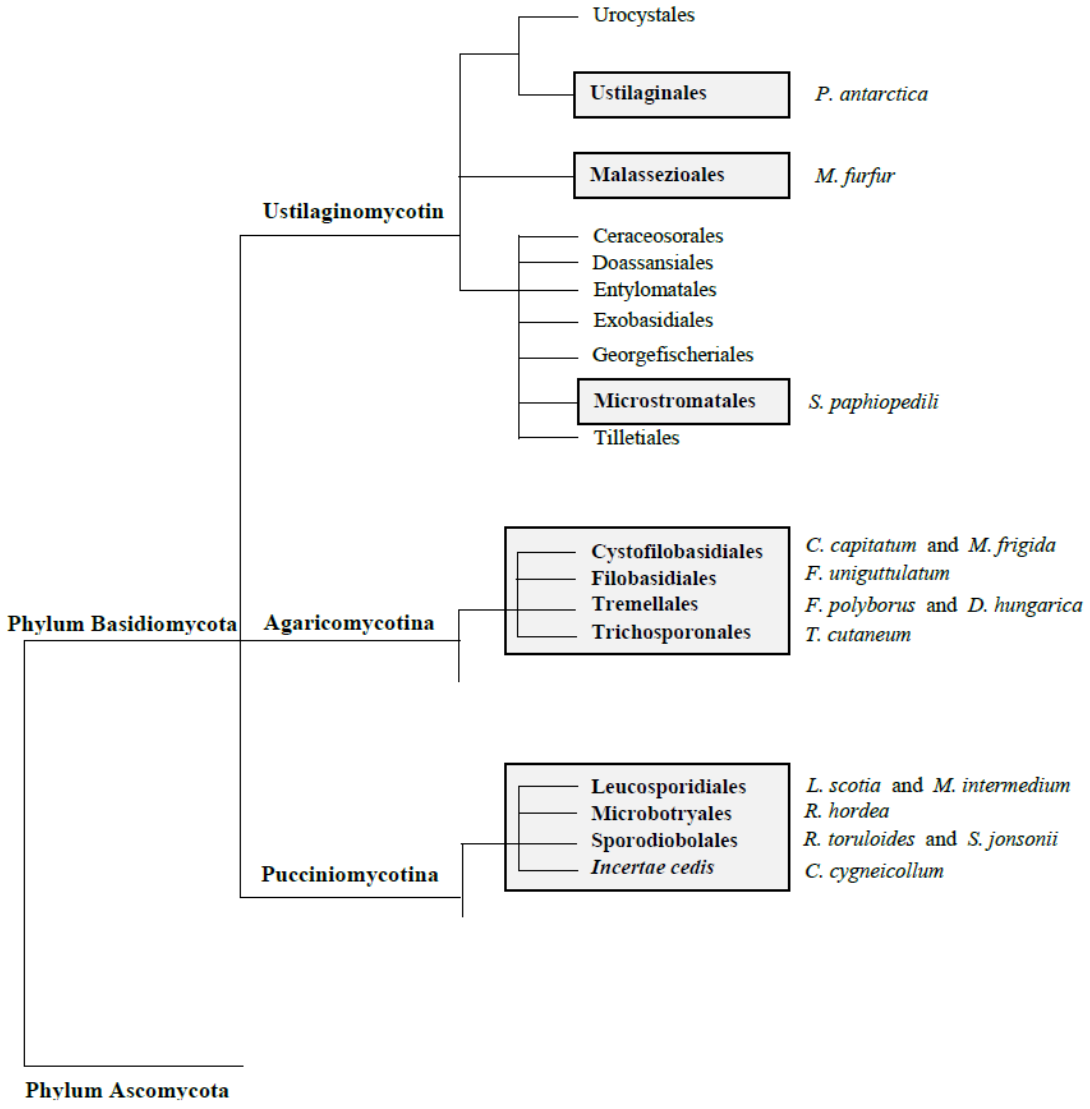

Figure 1. A diagram showing relative taxonomic positions of the ustilaginomycetous yeasts mentioned in this study.

steps, it becomes significantly different among eukaryotes, including the yeast species, because of the expression of various genes which generates diversity in *N*-linked glycan structures (Gemmill and Trimble, 1999). Consequently, the size, components, and branching patterns of mature glycans differ among different types of cell, tissue, and species (Kornfeld and Kornfeld, 1985; Paulson and Colley, 1989).

Majority of the total cellular and secreted proteome is composed of glycoproteins (Apweilaer et al., 1999; Jung et al., 2001). Proteins are complex biomolecules which perform essential functions necessary to support life. These proteins may either function as enzymes that mediate metabolic processes within the cell or as structural proteins that provide integrity and support to cellular structures. Proteins are produced in the cell in a pre-determined fate due to the fact they are encoded by another class of biomolecules called the deoxyribonucleic acids (DNA) which make up the genes that store the molecular information. Through a series of post-translational processing and in addition to proper folding, the protein becomes functional. Different PTM events which are largely dependent on the dynamic interplay of enzymes and pathways result in the production of proper and functional proteins. Among these PTMs, glycosylation is expected to be the most abundant followed by phosphorylation, although phosphorylation has been experimentally found to be more common (Khoury et al., 2011).

The notion that phosphorylation represents the absolute experimental distribution does not necessarily indicate the relative levels of each of the other PTMs. This may be explained by the ease by which PTM analysis is carried out or the preference of the scientific community as

to which PTM to study (Khoury et al., 2011). Putatively, *N*-linked glycosylation is the most dominant PTM and therefore may have the most essential effect on the functionality of proteins and the biology of living organisms.

N-linked Glycosylation, Golgi α-mannosidase products and the Yeasts

N-linked protein glycosylation is present in all domains of life and has two characteristics in common: the oligosaccharide is preassembled on a lipid carrier and is then transferred *en bloc* to an *N* residue within the consensus sequence (*N-X-(S/T)*) of the protein where *X* is any other amino acid. Molecular mechanisms of *N*-linked glycosylation have been well-studied in several model eukaryotes such as human, plants, insects and yeasts. *N*-linked glycosylation, especially the strongly conserved early steps, is found in the eukaryotic domain (Kukuruzinska, 1998). The later steps in *N*-linked glycosylation are significantly different not only among eukaryotes but also among yeast species. The expression of different *N*-linked glycosylation related genes may generate diversity in *N*-linked glycan structures in these yeast species (Gemmill and Trimble, 1999). In mature glycans, therefore, the size, components, and branching patterns of glycans differ among the different types of cell, tissue and species (Kornfeld and Kornfeld, 1985; Paulson and Colley, 1989). In the case of yeasts, as it is in other eukaryotic organisms, *N*-linked glycosylation starts with an isoprenoid lipid dolichol which serves as a carrier of the oligosaccharide and localizes the biosynthetic pathway to the membrane of the endoplasmic reticulum (ER). Dolichol pyrophosphate (Dol-PP) is synthesized by *cis*-prenyl transferase, starting from farnesyl pyrophosphate and the sequential addition of C_5 isoprenoid units (Welti, 2012). This process

proceeds through the assembly of a $Glc_3Man_9GlcNAc_2$ (where Glc: glucose, Man: mannose, and GlcNAc: *N*-acetylglucosamine) oligosaccharide as a lipid-linked moiety with dolichol pyrophosphate resulting in the formation of the $Glc_3Man_9GlcNAc_2$Dol-PP (Burda and Aebi, 1999). A multisubunit protein complex, the oligosaccharyltransferase (OST), in the ER membrane of eukaryotes, transfers this oligossachariride glycoprotein precursor *en bloc* to *N* residues on proteins during translation resulting in the formation of glycosylated peptide chain. Following the covalent *en bloc* attachment of the oligosaccharide from the Dol-oligosaccharide precursor to *N* residues, a series of processing reactions occur. The first several steps resulting in an oligosaccharide precursor that is linked to the asparagine residue appear to be conserved among eukaryotic cells. These steps are depicted in Figure 2. Furthermore, in the ER, glucosidases I and II first act on the protein-linked oligosaccharide precursor to remove all three glucoses sequentially. An ER-located α1-2 mannosidase then cleaves a mannose residue. Afterwhich, these *N*-linked glycans become available for further trimming or extension by glycosylhydrolases and glycosyltransferases, respectively (Aebi, 2013; Varki et al., 1999; Aebi et al., 2009). Golgi enzymes play a key role in determining the synthesis of the various types of glycans. The order of action of the enzymes is reflected in their position in the Golgi stack which is composed of the *cis*-face, *medial*-face and the *trans*-face compartments. The Golgi receives a newly synthesized glycoprotein from the ER, which enters the Golgi at the *cis*-face that houses certain mannosidase I. On its passage to the *medial*-face, the glycan is subjected to the action of GlcNAc transferases while in the *trans*-face, the glycan is processed in an assembly line by certain glycosidases and glycosyltransferases such as galactosyltransferase and sialyltransferase (Reyes and Orellana, 2008; Cubero et al., 2008; Schoberer and Strasser, 2011).

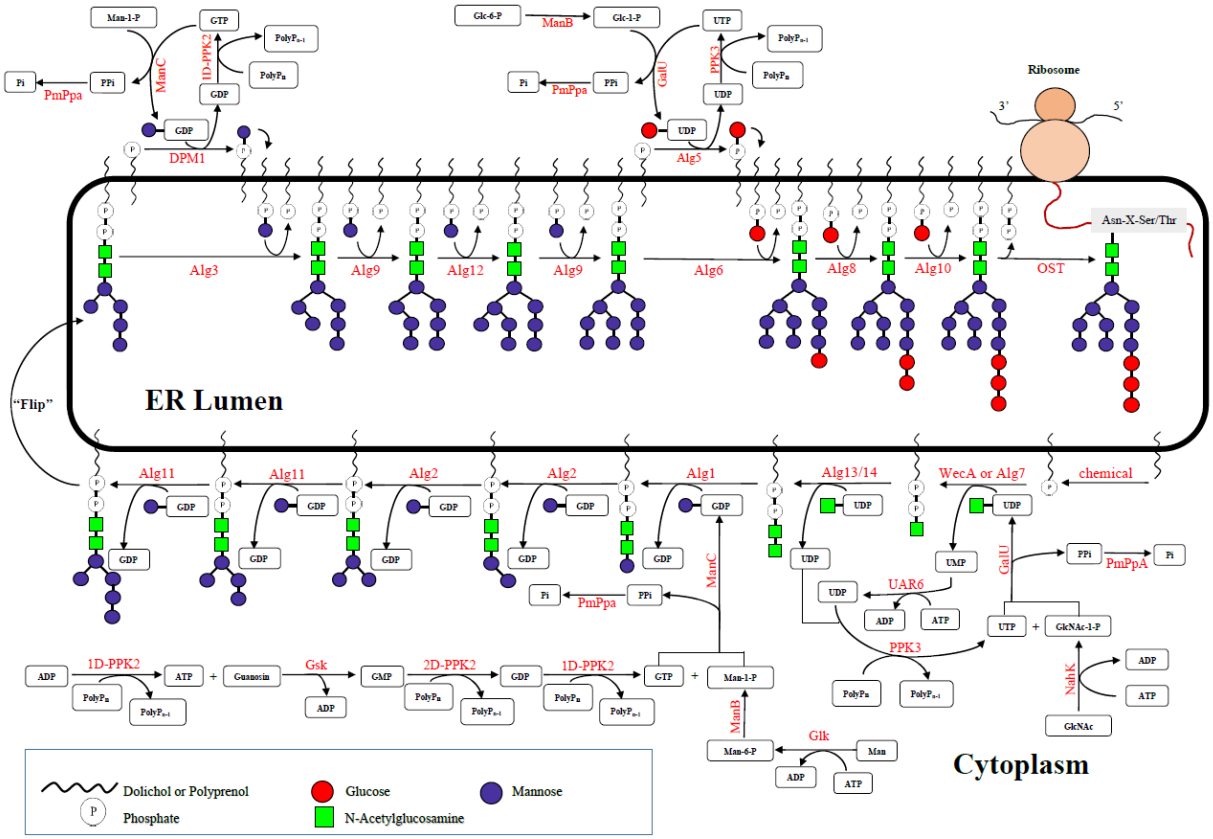

Figure 2. A visual representation of the early *N*-linked glycosylation steps showing various stages of glycan assembly leading to *en bloc* transfer to an asparagine. The early *N*-linked glycosylation steps are thought to be conserved in eukaryotes.

Primary examination of glycan structures in certain basidiomycetous mushrooms had also been carried out. *N*-linked glycosylation of certain yeast species belonging to the phylum Ascomycota has been well-studied as compared to yeasts belonging to the phylum Basidiomycota. *N*-linked glycan structures present in most of the basidiomycetous yeasts species, with the exception of *C. neoformans,* were not well characterized. Therefore, the creation of baseline *N*-linked glycan structure information for basidiomycetous yeasts is warranted. *Saccharomyces cerevisiae* (Ascomycota) produces *N*-linked glycans containing mannoses in the non-reducing terminal while *Schizosaccharomyces pombe* (Ascomycota) is characterized by the addition of galactose residues in the non-reducing terminal (Kukuruzinska et al., 1987; Zeigler et al., 1994). Cell walls and *N*-linked glycans of some *Candida* species (Ascomycota) such as *C. albicans,* a commensal organism in mucosal surfaces under normal conditions, have been found to contain β-mannans not previously found on the other yeast species described above (Suzuki and Fukuzawa 1982; Fukuzawa et al., 1995; Shibata et al., 1985). Figure 3 shows the hypermannosylated *N*-linked glycan structures of *S. cerevisiae* and *C. albicans* showing large numbes of mannoses. Functional analysis of the *och1* mutant of some medically relevant fungal pathogens, such as *C. albicans*, *Aspergillus fumigatus,* and *C. neoformans* demonstrated significant roles for the virulence of yeast-specific α1-6 mannose (Man)-containing polysaccharide (Kotz et al., 2010; Park et al., 2012; Leach and Brown, 2012). Cell wall glycan composition, *N*-linked phosphomannosylation and *N*-linked mannan branching was also found to have direct effect to cell wall structure and cell surface recognition, host defense mechanisms against *C. albicans,* macrophage migration and rate of phagocytosis (Mora-Montes et al., 2010; Lewis et al., 2012; McKenzie et al., 2010; Sheth et al., 2011).

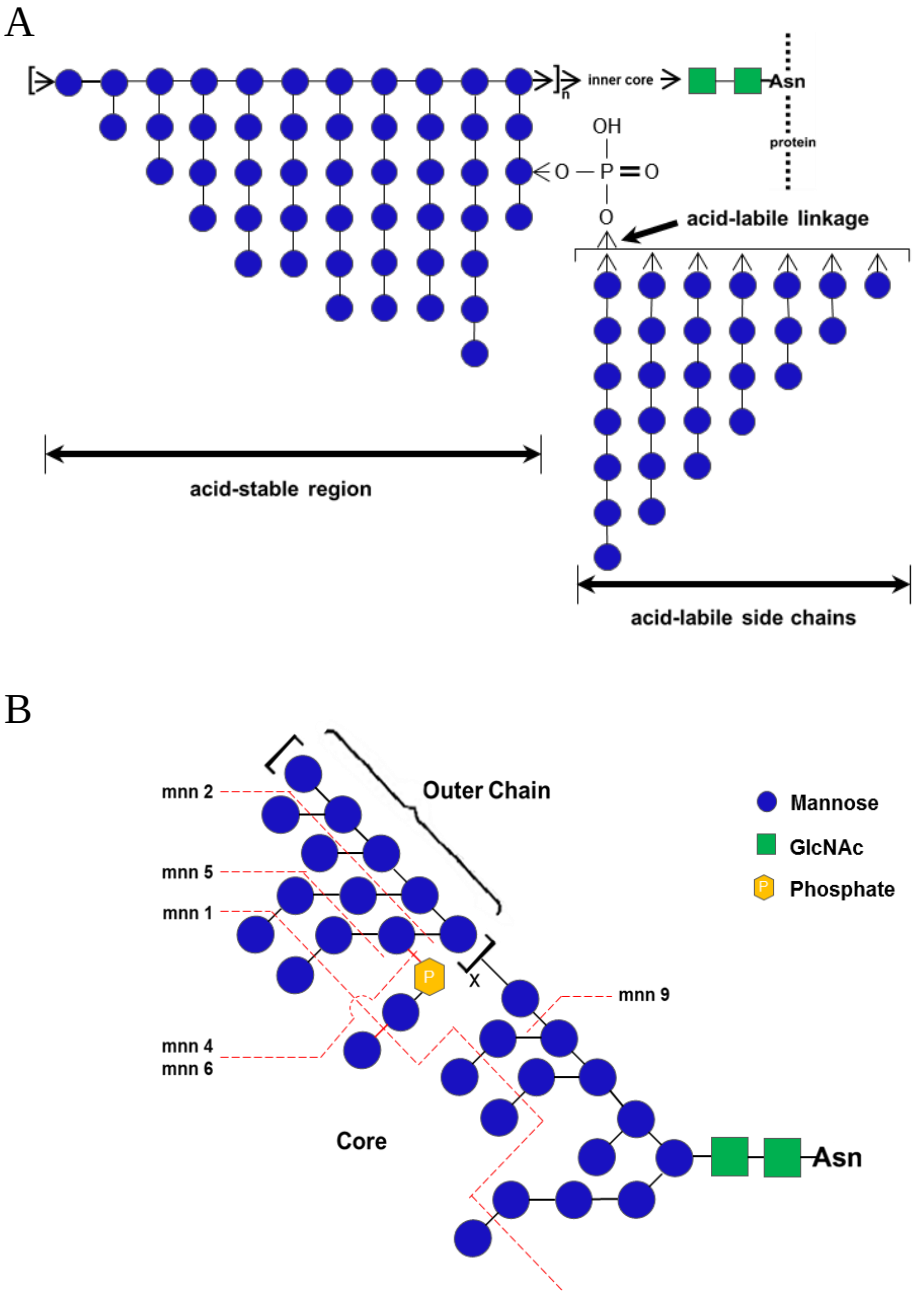

Figure 3. Structure of hypermannosylated *N*-linked glycans of (A) *C. albicans* and (B) *S. cerevisiae* showing large numbers of mannoses.

The Analysis of *N*-linked Glycosylation

The alteration of structure and the subsequent biological consequence, the physiological function of certain molecules and their distribution are just some of the standard tactics and features that were historically used to study glycans (Agard and Bertozzi, 2009). The foundations of genetics and biochemistry did not always result in the direct study of protein glycosylaton. The old notion that glycans are just simply decorations effectively hampered the propulsion of the era of glycomics in comparison to proteomics and genomics (Mariño et al., 2010). But with the advent of more modern technology in analyzing glycans, it has paved the way for the elucidation of the diverse functions and plethora of biological processes where glycans play important roles (Dwek, 1996). A number of analytical techniques including the use of different extraction and release techniques, flouresent labelling, chromatographic separation techniques, mass spectroscopy and nuclear magnetic resonance spectroscopy to name a few, are currently being used to revolutionize the way glycan analysis is done (Kotsias et al., 2019).

Different approaches are being used to improve the degree of quantification of *N*-linked glycans in biological samples. As a probable consequence of variations in the pre-processing stage of sample preparation, these analysis techniques often result in varied glycan profiles which is a challenge and at the same time, an opportunity for the development of better ways of glycan analysis (Mariño et al., 2010: Kotsias et al., 2019). In addition, the development of highly specific

lectins has led to the profiling of cell surface glycans and the subsequent correlations to disease as affected by different developmental stages (Feizi et al., 2003).

Current breath of knowledge of the *N*-linked glycan structures present in the Basidiomycetes has gained quite an attention especially in the past few years although their Ascomycetous counterparts are still more studied and engineered. *C. neoformans* is an example of a yeast species which had been studied more in depth compared to other species. *C. neoformans* unique xylosylated high-mannose type glycans and the corresponding biosynthetic pathways have been unraveled by Park et al. (2012) and Lee et al. (2014). Other basidiomycetous fungi have been studied such as *Coprinopsis cinerea* where high mannose glycans decorated with GlcNAc were found (Buser et al., 2009). Grass et al. (2009) discovered substitution by α1-6 mannose of α1-2 mannosyl residues of the canonical *N*-linked glycan precursor structure, aside from GlcNAc and fucose decorations in the basidiomycete *Cantharellus cibarius*. High mannose type *N*-linked glycans were also detected in *Schizophyllum commune*, a basiodiomycetous mushroom (Berends et al., 2009). The most recent account of a basidiomycetous yeast glycan analysis in published literature included in this dissertation which reports the *N*-linked glycans of 3 Ustilaginomycetous yeasts. This shall be the content of Chapters 2 and 3.

Significance, Objectives and Approach

Glycobiology is one of the current frontiers of biomolecular analysis, affected by challenges and complexity far beyond those in the proteomics and genomics fields. The basidiomycetous yeasts, in general, have not been well studied relative to their ascomycetous counterparts in terms of their glycosylation. This entire project including the contents detailed in this dissertation reconciles that fact that there is a disparity of the available knowledge of the glycosylation of the basidiomycetous yeasts as compared to other eukaryotic organisms. The representative yeasts discussed in this dissertation were chosen as subphylum Ustilaginomycotina, from among the other yeasts belonging to other subphylum, to serve as the initial baseline information for the analysis of the other basidiomycetous yeasts.

Determining the structures of *N*-linked glycans of basidiomycetous yeasts is a necessary first step in elucidating the various functionalities that *N*-linked glycosylation play. This may come handy in understanding their molecular roles in different biological processes. Functional glycomics key to the establishment of the putative and apparent connections between glycans and biological functions. To achieve these, glycan analysis must be done using standard and robust methods for glycan analysis. Similarities and differences in the glycan structure especially in the detailed terminal *N*-linked glycan structures might be implicative of the taxonomic position and evolutionary relatedness of certain taxa of the basidiomycetous yeasts since the relationship of glycan structure information to yeast diversity and taxonomy has not yet been fully explored yet. In order to relate glycan structural diversity with basidiomycetous yeast taxonomic positions,

analysis of the *N*-linked glycan structure and diversity in representative species of basidiomycetous yeasts is therefore warranted

This study aimed at analyzing the neutral *N*-linked glycans of some basidiomycetous yeasts that had never been subjected to detailed *N*-linked structural analysis before. Furthermore, this study discusses prospects borne by the extensive *N*-linked glycan structural analysis.

In general, the objectives are stated as follows:

- To determine the *N*-linked glycan structures in selected ustilaginomycetous yeasts *S. paphiopedili*, *P. antarctica* and *M. furfur*.
- To create baseline glycan diversity information.
- To relate the elucidated glycan structures to future scientific prospects.

The objectives of the study necessitate that glycoproteins are harvested from the cells of *S. paphiopedili*, *P. antarctica* and *M. furfur* post-cultivation using an appropriate medium and at optimal conditions. The maintenance for standard conditions for analysis is important to allow fidelity of interpretation and comparisons. The glycoprotein was then extracted, and the glycan moiety was cleaved, derived and processed before being subjected to a series of analyses. A battery of approaches such as high performance liquid chromatography (HPLC) using various stationary and mobile phases, glycosidase susceptibility, serial glycosidase digestion (i.e in the case of putative novel *N*-linked glycan structures), and liquid chromatography/ tandem mass spectrometry (LC/MS-MS) (Figure 4).

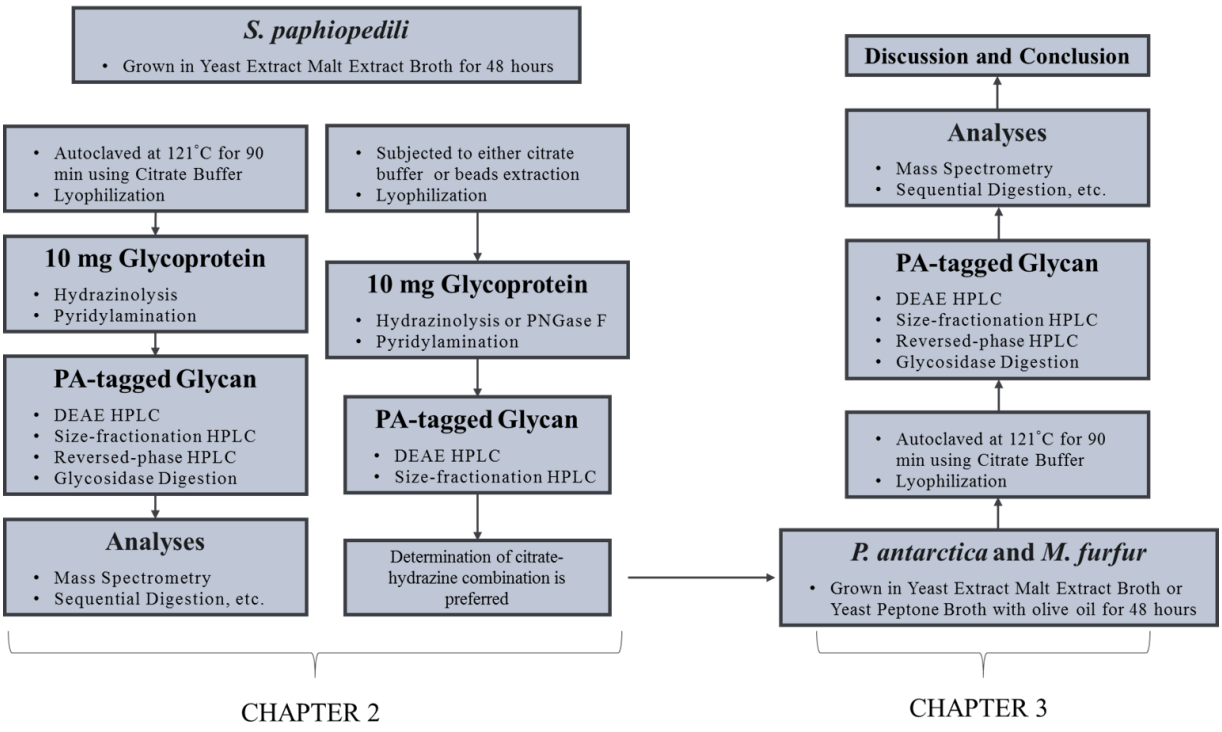

Figure 4. General strategy of investigation employed in this study.

Chapter 2

The Neutral *N*-linked Glycans of the Ustilaginomycete Yeast *Sympodiomycopsis paphiopedili*

INTRODUCTION

Sympodiomycopsis paphiopedili, a basidiomycetous type species classified under the class Microstromatales of subphylum Ustilaginomycotina was originally isolated as commensal yeast of *Paphiopedilum primurinum* orchid nectar in Japan (Sugiyama et al., 1991). It has been considered as potential yeast for biotechnological applications as it was found to secrete an extracellular glycolipid, a 2-15-16 trihydroxypalmitic acid to which a cellobioside is attached (Kulakovskaya et al., 2004). Yeast and mycelial fungi are susceptible to this glycolipid making it valuable for medical applications (Golubev et al., 2004). *S. paphiopedili* has a dominant yeast morph but it is also associated with having a mycelial morph. It has certain similarities with the ascomycetous dimorphic yeast *Sympodiomyces paruus* but the structure of septal pore and the sequence of 18s rDNA show it to be closer to Ustilaginales (Suh et al., 1993; Suh and Sugiyama, 1994).

Before one can begin to understand the particular roles that glycans play in the biology of strict commensals such as *S. paphiopedili*, analysis of the *N*-linked glycan structures is first. Future studies on identifying possible biological roles of high mannose type *N*-linked *S. paphiopedili* glycans are needed. This study, therefore, aimed to identify the *N*-linked glycan structures present which is an important step to better understand the *S. paphiopedili* glycobiology. However, it is also important to make an accurate representation of the structures due to the analytical process sensitivity. This may be solved by comparing the citrate buffer-hydrazinolysis glycoprotein extraction and glycan release methods to the other possible combinations of extraction and release.

It was found that the citrate buffer glycan extraction coupled with the hydrazinolysis glycan release was the best extraction-release combination as compared to other combinations tested.

The glycan structure Manα1-2Manα1-6(Manα1-3)Manα1-6(Manα1-2Manα1-2Manα1-3)Manβ1-4GlcNAcβ1-4GlcNAc (M8A) was found to be the most abundant type of glycan in this species followed by the Manα1-2Manα1-6(Manα1-2Manα1-3)Manα1-6(Manα1-2Manα1-2Manα1-3)Manβ1-4GlcNAcβ1-4GlcNAc (M9A) and the Manα1-6(Manα1-3)Manβ1-4GlcNAcβ1-4GlcNAc (M3B) glycans. These high mannose type glycans were detected in the neutral *N*-linked glycan fraction describes the first report on the analysis of the neutral *N*-linked glycan structures of the basidiomycetous yeast *S. paphiopedili*, which forms the initial *N*-linked glycan baseline information in *S. paphiopedili*. HPLC and LC-MS/MS analyses were performed following the extraction and processing of the neutral *N*-linked glycans.

MATERIALS AND METHODS

Yeast and Growth Media

Yeast strains of *S. paphiopedili* (NBRC 10260) and *S. cerevisiae* (NBRP BY4741) were obtained from the culture collection of the National Bioresource Research Center, NITE (Chiba, Japan) and the National Bio-Resource Project, MEXT (Japan). For 48 h at 24˚C, the yeast strains were sub-cultured in 10 mL Yeast Malt Broth (YMB). The contents of the *S. paphiopedili* and *S. cerevisiae* tubes were transferred aseptically onto 100 mL of YMB with 10% glycerol and 100 mL of YMB, respectively. Then, the flasks were incubated at 24˚C with shaking. After 72 h of incubation, the yeast cells were harvested via centrifugation at 6,000 rpm for 5 min. The pellet was subjected to glycoprotein extraction while the supernatant was discarded.

Preparation of PA-glycans

The yeast pellets were resuspended on citrate buffer (20 mM citrate-NaOH, pH 7.0) before subjecting to autoclave at 121˚C for 90 min (Ohashi et al., 2010). The released glycoproteins were then precipitated using methanol at 4˚C for 1 h. Methanol was discarded from the suspension via centrifugation before dissolving the glycoprotein pellets in hot water then subjected to dialysis and lyophilization. Hydrazinolysis using hydrazine anhydrate at 100˚C for 10 h was then utilized to release the *N*-linked glycans from the glycoprotein as previously described (Yoshizawa et al.,

1966). 2-aminopyridine (PA) was used to tag the glycans at the reducing end (Hase et al., 1978) before subjecting them lyophilisation and dissolving them in ultrapure water.

High Performance Liquid Chromatography

The PA-glycan samples were subjected to anion-exchange HPLC using a TSKgel DEAE-5PW column (7.5 mm x 75 mm, Tosoh, Tokyo) and ultrapure water adjusted to pH 9.0 using 20% aqueous ammonia as solvent A for equilibrating the HPLC column. The solvent B, 0.5 M acetic acid (adjusted to pH 9.0 using aqueous ammonia), was then increased to 100% over a period of 20 min at a flow rate of 1 mL/min. fractions since the human α1-acid glycoprotein has acidic sialylated glycans, the PA-glycans from human α1-acid glycoprotein (Sigma-Aldrich, MO, USA) were used as standard in determining the elution position of the neutral and acidic PA-glycan (Fournier et al., 2000). The flow-through fraction corresponding to neutral PA-glycans was collected, lyophilized, and subjected to normal-phase (NP) HPLC using TSK Amide-80 column (2.0 mm x 150 mm, Tosoh). In NP-HPLC, HPLC-grade acetonitrile was used as solvent C while 20 mM formic acid adjusted to pH 4.0 using aqueous ammonia was used as solvent D. At a flow rate of 0.2mL/min, the column equilibration was done using 100% of solvent D for 20 min, while the concentration of solvent C was linearly increased to 100% for 50 min.

Collected peaks in NP-HPLC were subjected to reversed-phase (RP) HPLC using a Cosmosil 5C18-AR-II waters column (4.6 mm x 250 mm, Nacalai Tesque, Kyoto, Japan). 0.02%

trifloruoacetic acid (TFA) in ultrapure water (solvent E) at a flow rate of 0.7 mL/min was used in column equilibration. The concentration of the 20% HPLC-grade acetonitrile in 0.02% TFA (solvent F) was increased to 20% for 50 min. Various high mannose type PA-glycan isomers of $Man_3GlcNAc_2$-PA to $Man_9GlcNAc_2$-PA (M3-M9 PA-glycans) (TakaraBio, Shiga, Japan), where GlcNAc is *N*-acetylglucosamine, were used as standards to determine the respective elution positions. HPLC analyses were done at 320 nm emission wavelength and 380 nm detection wavelength. After the RP-HPLC peaks were collected, the samples were lyophilized and dissolved in mass spectrometry-grade acetonitrile for mass spectrometric analysis.

Enzymatic Digestion

The PA-glycans were digested using Endoglycosidase H (New England Biolabs, Massachusetts, USA) according to the manufacturer's protocol or with 100 munits of jack bean α-mannosidase (Sigma-Aldrich, MO, USA) in 50 mM citrate-NaOH at pH 4.5 for 12 h at 30˚C. PA-glycans that did not co-elute with standard PA-glycans were digested with 2.5 munits α1-2 mannosidase (Seikagaku Co., Tokyo, Japan) in 100 mM acetate-NaOH at pH 5.0 for 16 h at 30˚C. The resultant peaks were digested separately with 40 munits α1-6 mannosidase (New England Biolabs) and 32 munits α1-2/1-3 mannosidase (New England Biolabs) according to the manufacturer's protocol.

Mass Spectrometry Analysis

The PA-glycan isomeric forms collected from the RP-HPLC analyses were subjected to LC-MS/MS using an HCT plus ion-trap mass spectrometer (Brucker Daltonics, Bremen, Germany) with the Agilent Technologies 1200 HPLC Series (Agilent Technologies, Santa Clara, CA, USA). Ten picomoles each of the collected isomers were dissolved in MS-grade acetonitrile to yield a total of 50 µL. The mobile phase used for the LC analysis was composed of acetonitrile/acetic acid (solvent G: 98/2, v/v) and water/acetic acid/triethylamine (solvent H: 92/5/3, v/v/v). The PA-sugar chain was separated using a Shodex Asahipak NH2P-50 2D column (2.0 mm x 150 mm, Showa Denko Co., Ltd., Tokyo, Japan) by increasing the solvent H concentration from 20% to 55% over 35 min at the flow rate of 0.2 mL/min. The MS/MS parameters were as follows: scan range of 350 – 2750 mass to charge ratio *(m/z)*; nebulizer flow of 5.0 psi; dry gas flow rate of 3.0 L/min; dry temperature of 100˚C; target count of 200,000; and MS/MS fragmentation amplification of 1.0 V in the positive-ion mode.

RESULTS AND DISCUSSION

Separation of citrate extracted-hydrazine released PA-glycans using anion-exchange HPLC and NP-HPLC revealed the presence of glycans of various sizes.

Structurally complex glycans were rendered from the glycans of acidic group (such as phospates and pyruvates) produced by yeast species (Gemmill and Trimble, 1999). The separation by anion-exchange HPLC to obtain PA-glycans from *S. paphiopedili*'s glycoprotein is shown in Figure 5. Peaks were eluted within elution positions corresponding to monosialo, disialo and trisialo acidic glycans of the standard human α1-acid glycoprotein consisting of one, two and three sialic acid residues, respectively (Fournier *et al.,* 2000). Based on the co-elution of the acidic fractions of the standard human α1-acid glycoprotein within elution time, these peaks may be presumed to be acidic. Since the structures of neutral *N*-linked glycans are relatively less complicated and simpler to understand compared to their acidic counterparts, flow through fractions of neutral glycans were detected and subjected to succeeding analyses to provide initial baseline information. This fraction was the portion that eluted at 0 position in Figure 5. The fractions containing neutral PA-glycan were collected, freeze-dried, dissolved and further separated in NP-HPLC alongside with the standard $Man_{3\text{-}9}GlcNAc_2$-PA glycans (Figure 6). Table 1 presented the standard PA-glycans and their determined structures. The presumptive neutral $Man_{3\text{-}9}GlcNAc_2$-PA-sized glycans were the first subjects of further analysis since they were represented by major and well-separated peaks in NP-HPLC. The higher-sized glycans eluted after the standard PA-glycans are the potential hypermannosylated glycans.

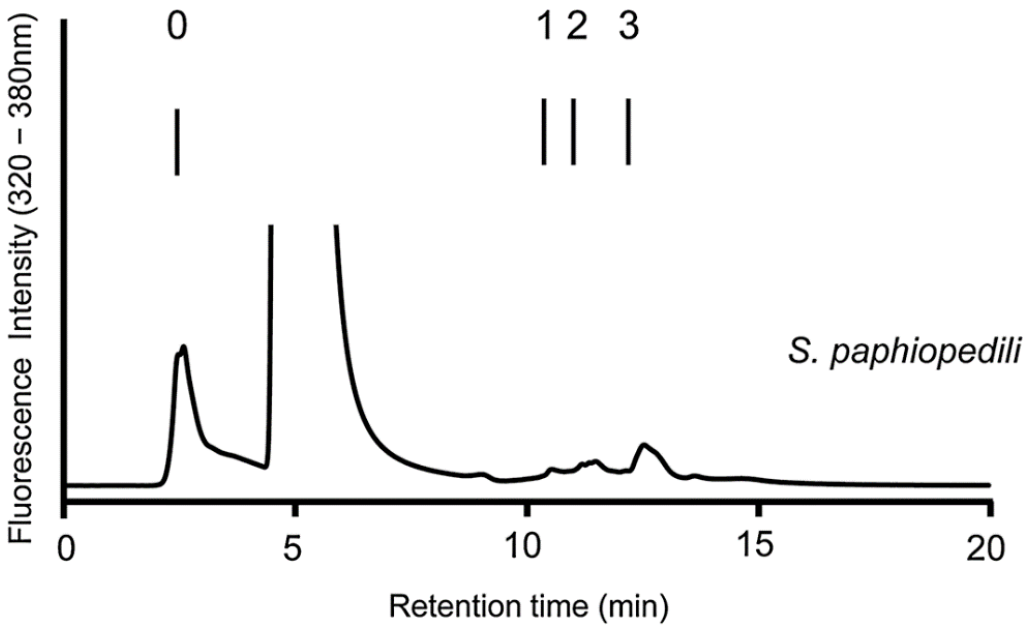

Figure 5. Anion-exchange HPLC (at 320 nm emission and 380 nm detection wavelengths) of PA-glycans from *S. paphiopedili.* PA-glycans were separated by DEAE anion exchange-HPLC. PA-glycans from human *α*1-acid glycoprotein were used as the standard. The numbers and lines show the elution positions of standard PA-glycans containing zero to three sialic acid residues. Peak eluting at 0 position was collected for further analyses.

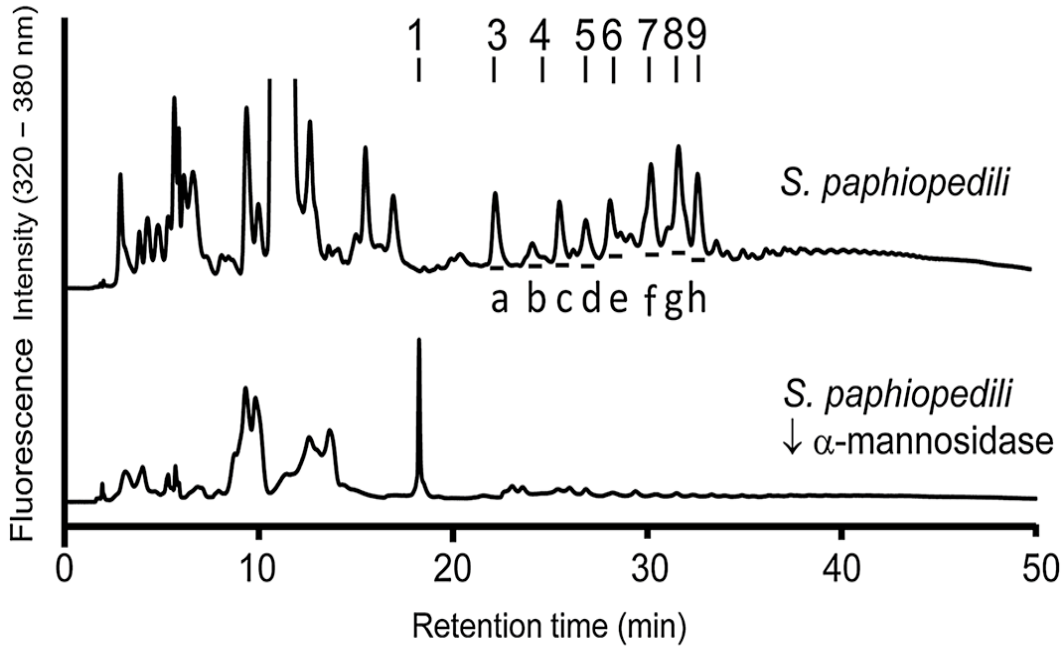

Figure 6. Normal-phase HPLC (at 320 nm emission and 380 nm detection wavelengths) of neutral PA-glycans. Neutral PA-glycans from anion-exchange chromatography were separated by normal-phase (NP) HPLC. Peaks eluting closely to standard $Man_{3–9}GlcNAc_2$-PA glycans were collected, labelled and lyophilized for further analysis. The numbers (1–9) on the chromatogram indicate the elution positions of standard M1-, M3-, M4-, M5-, M6-, M7-, M8- and M9-PA glycans. Jack bean *α*-mannosidase-digested peaks are also shown alongside the undigested sample.

Table 1. The standard PA-glycans and their structures.

PA-glycan and structure	PA-glycan and structure
M3B-PA Manα1—6 Manβ1—4GlcNAc β1—4GlcNAc—PA Manα1—3	M7A-PA Manα1—2 Manα1—6 Manα1—3 Manα1—6 Manβ1—4GlcNAc β1—4GlcNAc—PA Manα1—2 Manα1—3
M4B-PA Manα1—6 Manα1—3 Manα1—6 Manβ1—4GlcNAc β1—4GlcNAc—PA	M7B-PA Manα1—6 Manα1—3 Manα1—6 Manβ1—4GlcNAc β1—4GlcNAc—PA Manα1—2 Manα1—2 Manα1—3
M5A-PA Manα1—6 Manα1—3 Manα1—6 Manβ1—4GlcNAc β1—4GlcNAc—PA Manα1—3	M8A-PA Manα1—2 Manα1—6 Manα1—3 Manα1—6 Manβ1—4GlcNAc β1—4GlcNAc—PA Manα1—2 Manα1—2 Manα1—3
M6A-PA Manα1—2 Manα1—6 Manα1—3 Manα1—6 Manβ1—4GlcNAc β1—4GlcNAc—PA Manα1—3	M8B-PA Manα1—2 Manα1—6 Manα1—3 Manα1—6 Manβ1—4GlcNAc β1—4GlcNAc—PA Manα1—2 Manα1—3 Manα1—2 Manα1—3
M6B-PA Manα1—6 Manα1—3 Manα1—6 Manβ1—4GlcNAc β1—4GlcNAc—PA Manα1—2 Manα1—3	M9A-PA Manα1—2 Manα1—6 Manα1—3 Manα1—6 Manβ1—4GlcNAc β1—4GlcNAc—PA Manα1—2 Manα1—3 Manα1—2 Manα1—2 Manα1—3
M6C-PA Manα1—6 Manα1—3 Manα1—6 Manβ1—4GlcNAc β1—4GlcNAc—PA Manα1—2 Manα1—3	

Analysis of differently-extracted and released *N*-linked glycans revealed similar range of size with the citrate buffer-hydrazine combination employed in this study.

Glycoprotein samples that were subjected to a variety of extraction and release treatments (citrate buffer or glass beads extraction coupled with either hydrazinolysis or PNGase F glycan release) resulted in less varied *N*-linked glycan peaks appearance (Figure 7B) as compared with the original citrate-hydrazine treatment (Figure 7A and Figure 5). However, except for the marked difference in the relative proportions of the peaks, there was no apparent change in the size ranges among the citrate extracted-hydrazine released (CH), citrate extracted-PNGase F released (CP), beads extracted-hydrazine released (BH) or beads extracted-PNGase F released (BP) neutral *N*-linked glycans falling within the standard PA-glycan standard sizes (Figure 7). This means that the citrate buffer extraction-hydrazine glycan release is the best combination from among the other combinations tested. A similar analysis on the effect of glycoprotein extraction and release protocol was done on *S. cerevisiae* yeast cells. Figure 8 shows that most of the peaks corresponding to the high mannose as well as the minor hypermannosylated *N*-linked glycan were also susceptible to Endoglycosidase H suggesting that these contained *N*-linked glycans while the peaks eluted earlier (around 10-12 min) corresponding to non-*N*-linked glycans were not susceptible to Endoglycosidase H. This is due to the fact that the bond between the chitobioses of the core *N*-linked glycan structure is cleaved by Endoglycosidase H possessing at least 3 mannose residues, one of which is an α1-3 mannose residue attached to an α1-6 mannose residue (Maley et al., 1989). Endoglycosidase H typically acts on high mannose, hybrid *N*-linked but not bi-, tri-, tetra- or pentaantennary (complex) chains (Trimble and Tarentino, 1991).

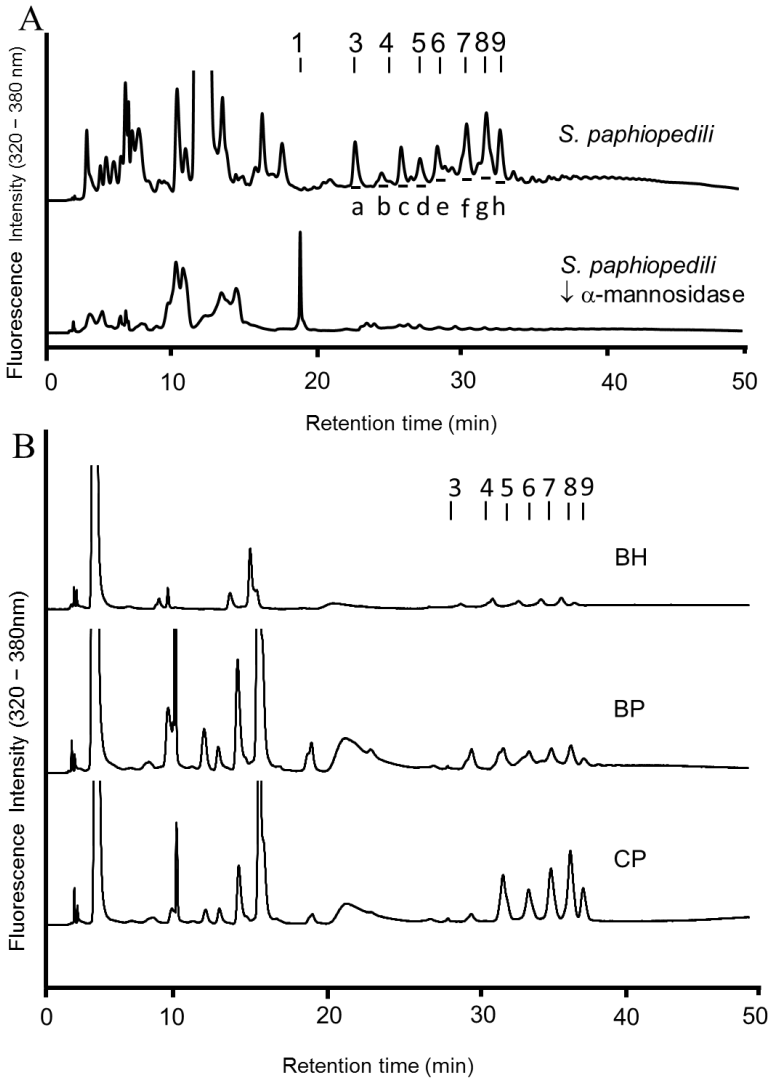

Figure 7. (A) Range of peaks of *S. paphiopedili* with CH (Citrate Buffer-Hydrazine) (B) Differently extracted and released neutral PA-glycans of *S. paphiopedili* on NP-HPLC. Citrate extracted–PNGase F-released (CP), bead-extracted–hydrazine-released (BH) or bead-extracted–PNGase F-released (BP) neutral PA-glycans of *S. paphiopedili* were separated by NP-HPLC (at 320 nm emission and 380 nm detection wavelengths). The numbers (3–9) on the chromatogram indicate the elution positions of standard M3-, M4-, M5-, M6-, M7-, M8- and M9-PA glycans.

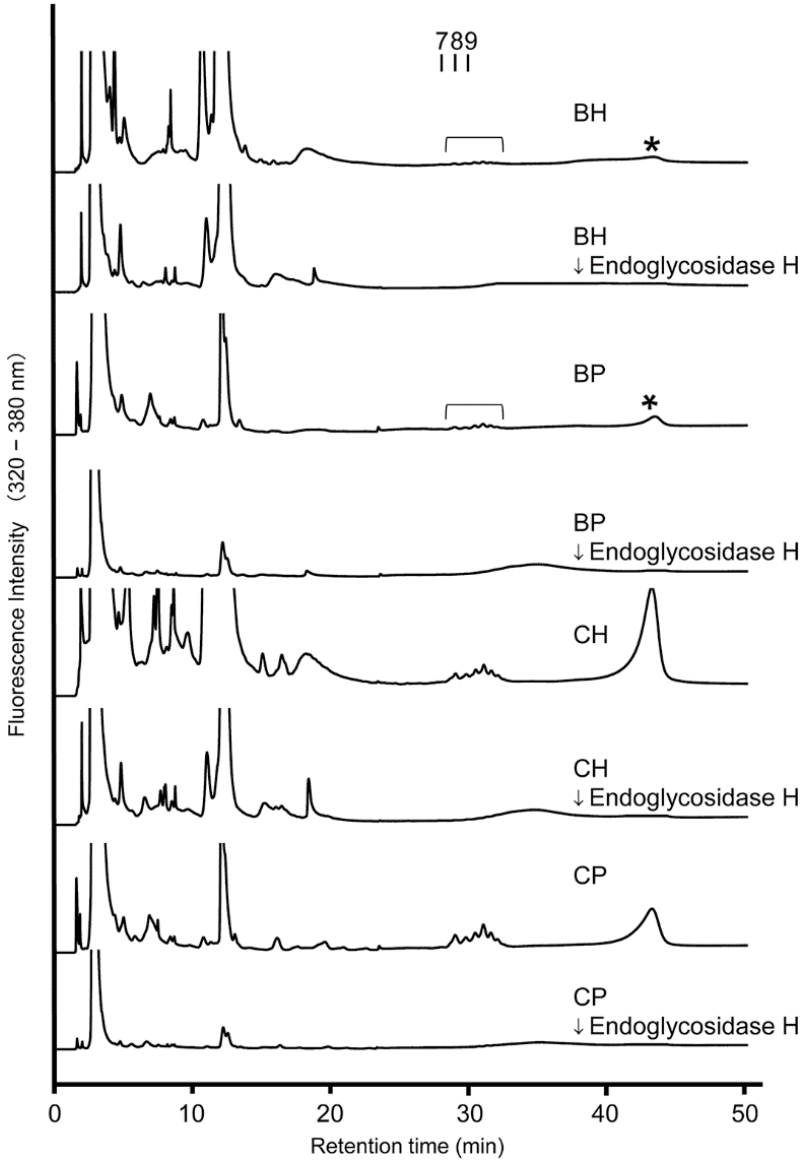

Figure 8. Normal-phase HPLC (at 320 nm emission and 380 nm detection wavelengths) of differently extracted and released neutral PA-glycans and PA-glycans digested with Endoglycosidase H of *Saccharomyces* released (CP), bead-extracted–hydrazine-released (BH) or bead-extracted–PNGase F-released(BP) neutral PA-glycans of *S. cerevisiae* were separated by NP-HPLC. The samples were also digested with Endoglycosidase H, indicating that these peaks were composed of *N*-linked glycans. The numbers (7–9) on the chromatogram indicate the elution positions of standard M7-, M8- and M9-PA-glycans while the brackets and asterisks denote the position of the high mannose and hypermannosylated glycan peaks of CP- and CH-treated *S. cerevisiae*, respectively.

In addition, Figure 8 shows the glycan peak yields eluted around the standard M7-M9 PA-glycan positions (denoted below the bracket) as well as possible hypermannosylated glycans (denoted below the asterisk) of the BH- and BP-treated *S. cerevisiae* were obviously lower than those of CH- and CP-treated samples as shown in the NP-HPLC chromatogram peak sizes. This shows that citrate buffer extraction of glycoprotein coupled with hydrazine release of glycans results in the highest glycan peak yield among the combination of methods used. Furthermore, the Endoglycosidase H susceptible-high mannose type and possible hypermannosylated glycans were detected in all the CP-, CH-, BP- and BH- treated *S. cerevisiae N*-linked glycan samples. This suggests that the use of citrate buffer coupled with hydrazine is the best glycoprotein extraction-glycan release method combination from among the others tested, as shown by the highest glycan peak yield and similarly-ranged glycan peaks compared to the other glycoprotein extraction and release combinations (Figures 7 and 8).

Jack bean α-mannosidase digestion confirmed that α-linked mannoses are attached to the *N*-linked glycans.

There are 8 *S. paphiopedili* major peaks in Figure 5 were collected and designated accordingly as s-a, s-b, s-c, s-d, s-e, s-f, s-g, and s-h. Those peaks were eluted at positions close to the standard $Man_{3\text{-}9}GlcNAc_2$-PA glycans. Jack bean α-mannosidase, an enzyme with the ability to cleave the α1-2, α1-3 and α1-6 Man linkages in the non-reducing terminal of the glycans, was used to confirm if the peaks contain α-linked Man residues at the non-reducing end (Li, 1967; Snaith and Levvy, 1968). The PA-glycan peaks eluted slower than $Man_3GlcNAc_2$-PA were digested

resulting in the elution of the digested glycan at the $Man_1GlcNAc_2$-PA (M1 PA-glycan) position after treatment with jack bean α-mannosidase (Figure 5). To determine the elution position of the M1 PA-glycan, jack bean α-mannosidase-digested $Man_9GlcNAc_2$-PA was used as glycan standard. Since most of the peaks were eluted at the M1 PA-glycan position, it can be considered that the non-reducing ends of the PA-glycans are made up of α-linked Man residues. The higher sized glycans eluted after the standard PA-glycans were also susceptible to jack bean α-mannosidase. Based on the number of jack bean α-mannosidase-susceptible minor peaks eluted after the standard PA-glycans, the hypermannosylated *N*-linked glycans can be presumed to contain at least 25 mannose residues

Reversed-phase HPLC revealed the presence of isomeric forms while mass spectrometry determined the molecular masses.

To separate different isomeric forms, NP-HPLC-collected PA-glycans were subjected to RP-HPLC. As shown on Figure 9, some of the NP-HPLC peaks of *S. paphiopedili* are composed of various isomeric forms. The presumptive structures of these abundant glycans were assigned based on their co-elution with standard PA-glycans in both NP-HPLC and RP-HPLC. However, some peaks did not co-elute exactly with the standard PA-glycans and were therefore subjected to additional glycosidase digestion analyses to determine their presumptive structures.

In order to identify the individual component sugars of the RP-HPLC-isolated peaks corresponding to the *m/z* of the fragments generated, LC-MS/MS analysis was performed. Moreover, the mass spectrometry data were used as basis to determine the *m/z* of fragments of the peaks that were susceptible to jack bean α-mannosidase but did not co-elute exactly with the standard PA-glycans in the previous HPLC analyses (Figure 10). Fragmentation pattern and *m/z* determined the composition of the different PA-glycan isomers analyzed.

The full length of presumptive $Man_4GlcNAc_2$-PA glycans (peak s-rb1 and peak s-rc1) resulted to an *m/z* of 1151.8 $[M+H]^+$ wherein each preceding generated fragment ion corresponds to a loss of one hexose residue with *m/z* of 503.1 corresponding to the GlcNAcβ1-4GlcNAc-PA (Figure 10A and 10B). The full length of presumptive $Man_6GlcNAc_2$-PA glycans (peak s-re1 and s-re2) yielded an *m/z* of 1476.2 $[M+H]^+$ wherein each preceding generated fragment ion corresponds to a loss of one hexose residue with *m/z* of 503.1 corresponding to the GlcNAcβ1-4GlcNAc-PA (Figure 10C and 10D). Based on the results of the mannosidase digestions of PA-glycan samples, HPLC analyses, and mass spectrometry, it can be concluded that the *N*-linked glycans of *S. paphiopedili* are of the high mannose type and range from $Man_{3\text{-}9}GlcNAc_2$ with the M8A glycan (24%) being the major structure, followed by the M9A and M3B glycans both at 10% each as computed using their relative peak area size. The various peak designations, glycan identities, elution time, *m/z* and percentage abundance were shown in Table 2 while Figure 11 shows the various structures determined for the glycan peaks which co-eluted with the standard PA-glycans.

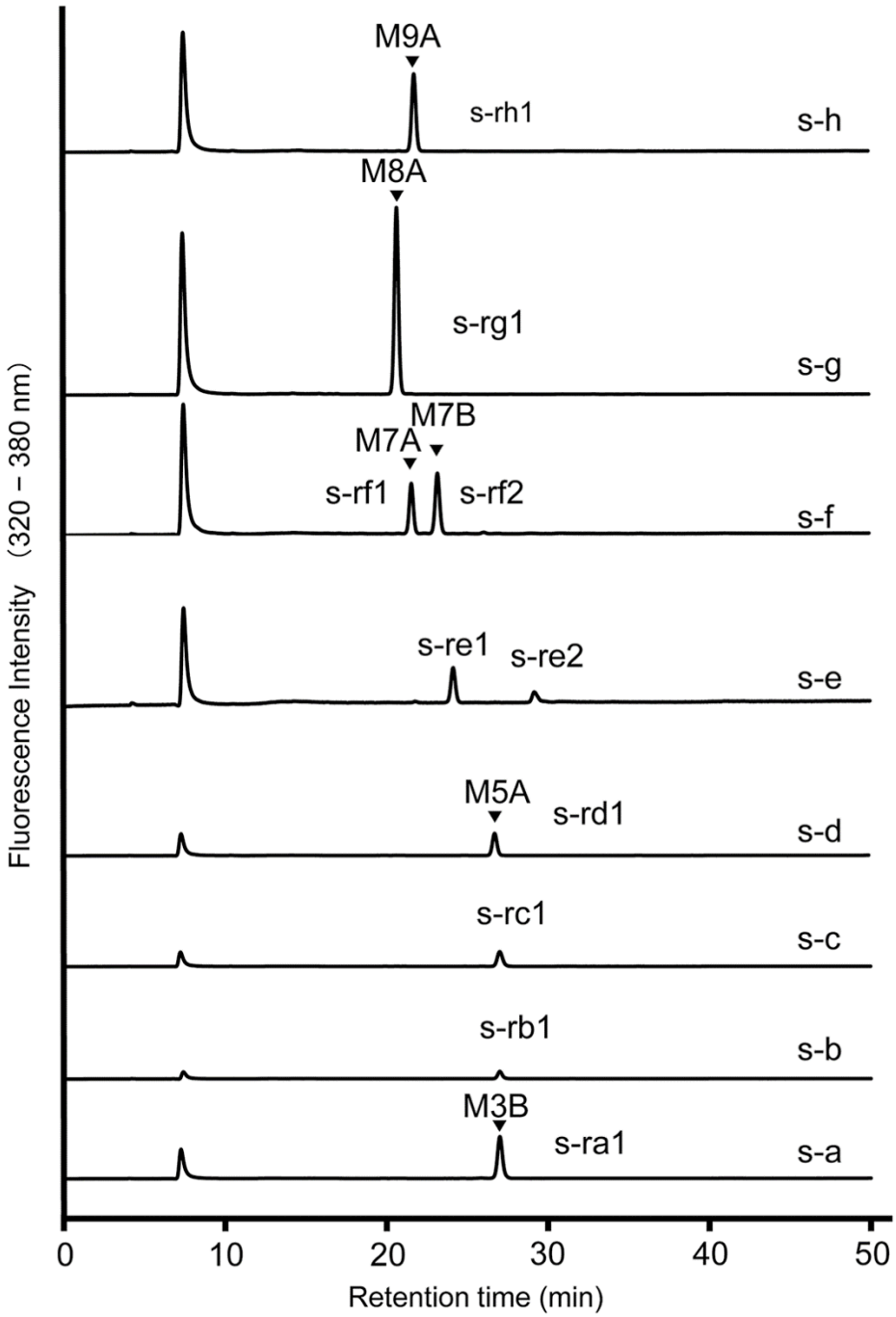

Figure 9. Reversed-phase (RP) HPLC (at 320 nm emission and 380 nm detection wavelengths) of peaks s-a to s-h. Peaks s-a to s-h isolated from NP-HPLC were further separated by RP-HPLC. The arrows in the chromatograms show the elution positions of standard PA-glycans.

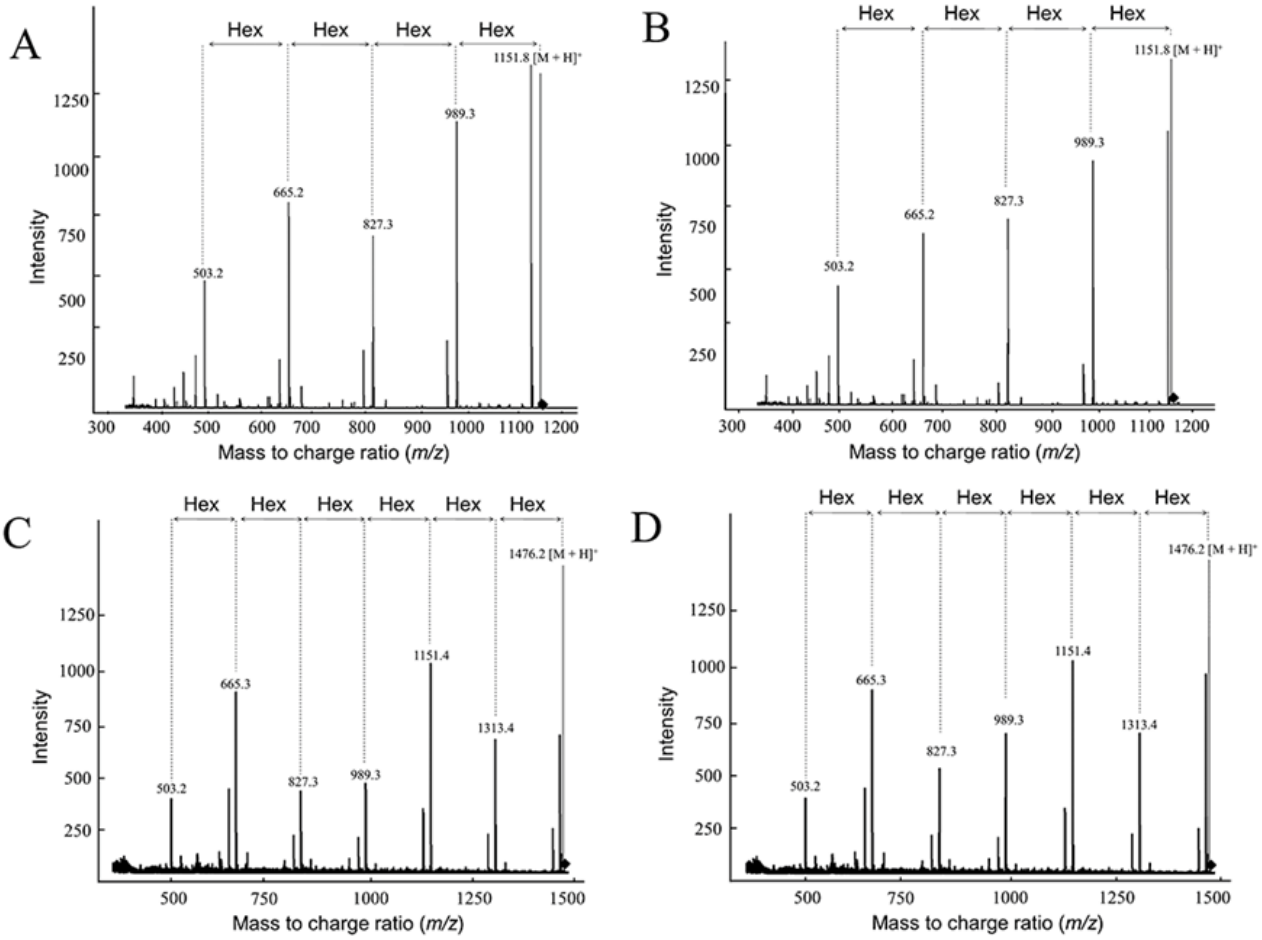

Figure 10. Mass spetrometric analysis of the peaks that did not co-elute with the standards in HPLC. Mass spectrometric data show that fragmentation results in one loss of hexose. The number of hexoses in the fragmentation pattern reveals the identity of the peaks presumptively identified in previous NP-HPLC and RP-HPLC analyses. Jack bean *α*-mannosidase digestion analysis confirms that the hexoses annotated in MS are mannoses. (A) Peak s-rb1; (B) peak s-rc1; (C) peak s-re1; and (D) peak s-re2. The rhombus (♦) indicates the *m/z* of the precursor ion. $[M + H]^+$ adduct ions were detected.

Table 2. Summary of detected properties of the neutral *N*-linked glycans of *S. paphiopedili.*

Peak	Composition	Elution Time (min) (NP-HPLC)	Elution Time (min) (RP-HPLC)	*m/z*	Identity	Abundance%
s-ra1	$Hex_3GlcNAc_2$	23.3	27.0	989.3	M3B	15
s-rb1	$Hex_4GlcNAc_2$	24.1	26.9	1151.8	M4*	3.9
s-rc1	$Hex_4GlcNAc_2$	26.5	27.1	1151.8	M4*	8.2
s-rd1	$Hex_5GlcNAc_2$	27.9	26.7	1313.8	M5A	8.8
s-re1	$Hex_6GlcNAc_2$	29.1	24.1	1476.2	M6**	5.4
s-re2	$Hex_6GlcNAc_2$	29.1	29.1	1476.2	M6**	1.6
s-rf1	$Hex_7GlcNAc_2$	31.2	21.5	1638.1	M7A	8.1
s-rf2	$Hex_7GlcNAc_2$	31.2	23.1	1638.1	M7B	10
s-rg1	$Hex_8GlcNAc_2$	32.6	20.6	1800.2	M8A	24
s-rh1	$Hex_9GlcNAc_2$	33.6	21.7	1962.5	M9A	15

***** Possible isomer other than M4B

** Possible isomers other than M6A or M6B

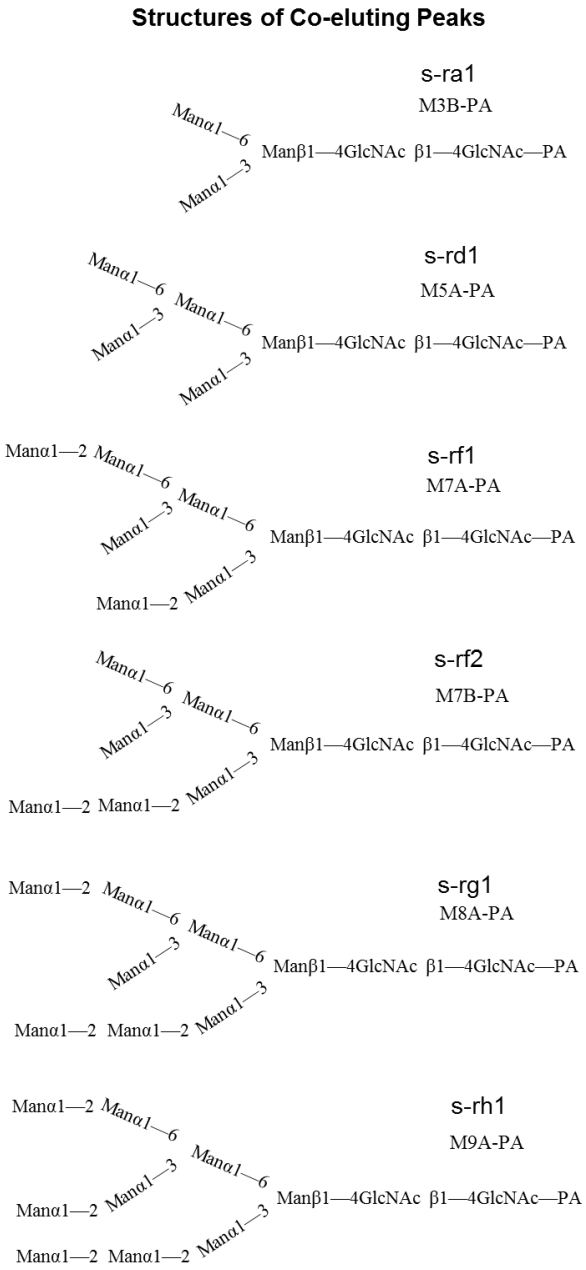

Figure 11. Abbreviations and proposed structures of the *N*-linked glycans peaks co-eluting with standard PA-glycans.

Cell wall glycans decorated with certain residues (e.g. mannose, galactose, galactofuranose, xylose or phosphate) had been found in fungi and yeasts belonging to Ascomycota and Basidiomycota (Gemmill and Trimble, 1999; Park et al., 2012; Deshpande et al., 2008; Buser et al., 2010). Previous investigations have shown that the presence or absence of certain monosaccharides and their ratio are valuable criteria in the chemotaxonomic and phylogenetic assignment of the yeast and yeast states of the members of the Ascomycota and Basidiomycota (Prillinger et al., 1991). Moreover, *N*-linked glycan diversity and abundance may be transient and stage-specific, as evidenced by the difference in the *N*-linked glycan populations between the mycelial and the fruiting bodies of a basidiomycete *Schizophyllum commune* (Berends et al., 2009). Thus, the differences in the glycan structure in mycelial stages of the yeast species studied are also intriguing. These may also have significance in future taxonomic and biological considerations of yeasts, especially for the dimorphic basidiomycetous yeasts species.

Structural analysis of peaks s-rb1, s-rc1, s-re1 and s-re2 by glycosidase digestions revealed some other possible structures.

Table 2 shows the peaks and relative abundances, including some peaks such as, s-rb1, s-rc1, s-re1 and s-re2, which did not match with standard PA-glycans in RP-HPLC. These glycans have been confirmed in LC-MS/MS to have hexoses (Figure 10) that may represent other possible isomeric forms of the standard glycans. As revealed by RP-HPLC and LC-MS/MS analysis, peaks s-rb1 and s-rc1 may identified as M4 glycans other than the M4B isomer while s-re1 and s-re2

may identified as M6 glycans other than the M6A, M6B or M6C isomers. These peaks were digested with α1-2 mannosidase, then with α1-2/1-3 mannosidase or α1-6 mannosidase in a successive manner in order to deduce their possible structures. Specifically, the digestion products of α1-2 mannosidase reactions were then digested separately by α1-2/1-3 mannosidase or α1-6 mannosidase (Figure 12) which cleaves α1-2/1-3 linked mannoses and unbranched α1-6 linked mannoses, respectively (Wong-Madden and Landry, 1995).

Using NP-HPLC, the peaks s-rb1 and s-rc1 which did not co-elute with the standard M4 PA-glycans were digested with α1-2 mannosidase and detected. The resultant peaks were collected and separately digested with α1-2/1-3 mannosidase and α1-6 mannosidase. In the case of the s-rb1 peak, an M3-sized PA-glycan peak (s-rb1a) was obtained after digestion with α1-2 mannosidase suggesting the presence of an α1-2 linked mannose. Peak s-rb1a yielded an M2-sized PA-glycan peak after digestion with α1-2/1-3 mannosidase indicating the presence of an α1-3 linked mannose.

However, peak s-rb1a was not susceptible to α1-6 mannosidase which suggests the possibility that it consists of an α1-6 mannose to which another α1-3 mannose is bound (Manα1-3Manα1-6Manβ1-4GlcNAcβ1-4GlcNAc-PA). The s-rc1 peak was not susceptible to α1-2 mannosidase which yields an M4-sized PA-glycan peak (s-rc1a). Peak s-rc1a was not susceptible to α1-6 mannosidase but was digested to an M2-sized PA-glycan peak by α1-2/1-3 mannosidase indicating the presence of two α1-2 mannoses. The α1-6 mannosidase enzyme was able to digest M4B PA- glycan under the same enzymatic conditions. On the other hand, the s-re1 and s-re2 which did not co-elute with the standard M6 PA-glycans had the same mannosidase digestion profile results. An M4-sized PA-glycan peak, in the case of the s-re1 peak (s-re1a), was obtained

after digestion with α1-2 mannosidase suggesting the presence of two α1-2 linked mannoses. The s-re1a peak produced an M2-sized PA-glycan peak when digested with α1-2/1-3 mannosidase which indicates the presence of two α1-3 linked mannoses but was not susceptible to α1-6 mannosidase after digestion. The results of the mannosidase digestion, together with the previous analyses were used to deduce the possible structures of the non-coeluting peaks. The proposed structures are presented in Figure 13.

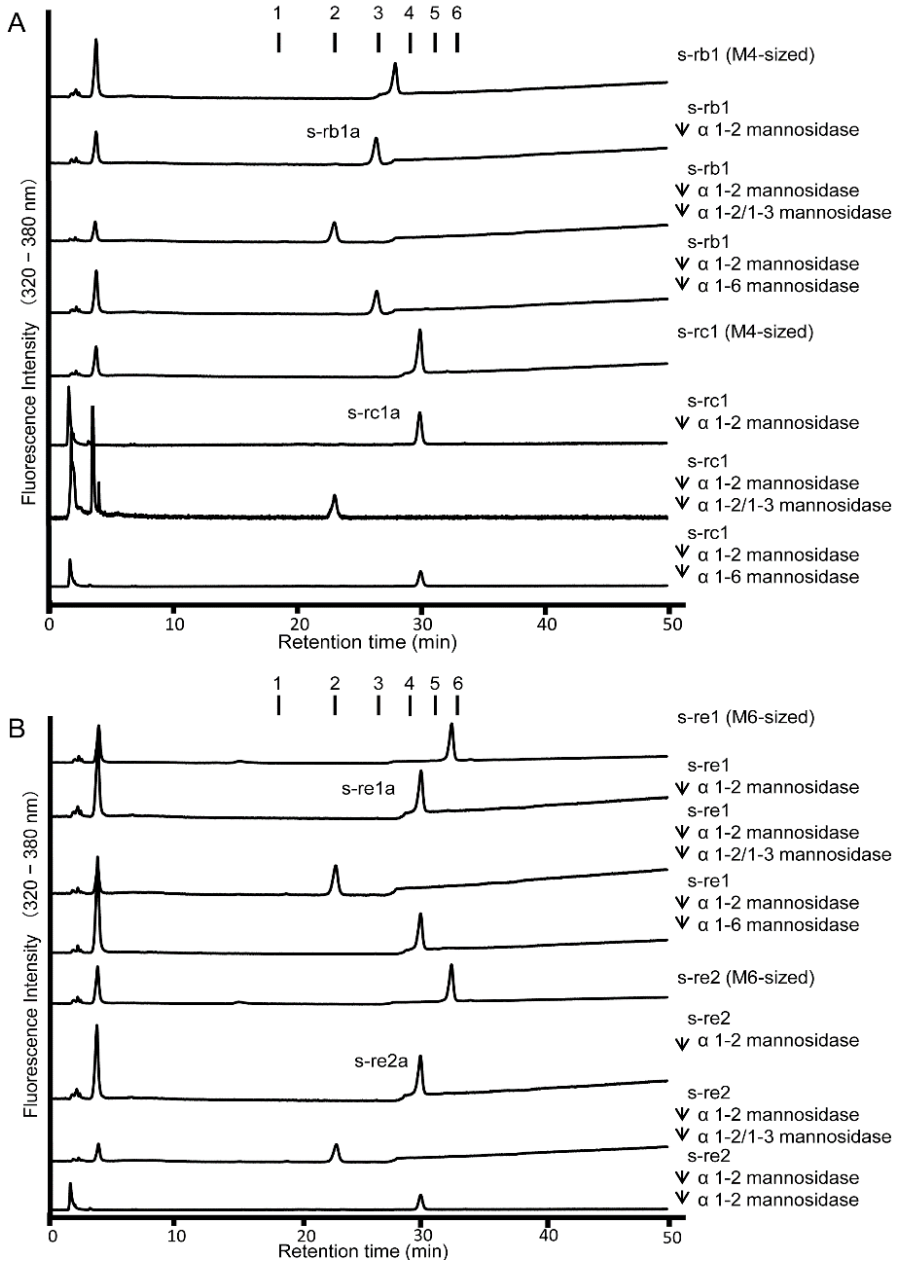

Figure 12. Sequential mannosidase digestion profile of unknown M4 and M6-sized glycan. The NP-HPLC (at 320 nm emission and 380 nm detection wavelengths) chromatogram of unknown (A) M4 peaks (s-rb1 and s-rc1) and (B) M6 peaks (s-re1 and s-re2) glycans digested with α1–2 mannosidases. The resulting glycan peaks were collected and each digested separately with α1–2/1–3 mannosidase or α1–6 mannosidases. The numbers (1–6) on the chromatogram indicate the elution positions of standard M1-, M2-, M3-, M4-, M5-, and M6-PA glycans. The proposed structures are shown in Figure 13.

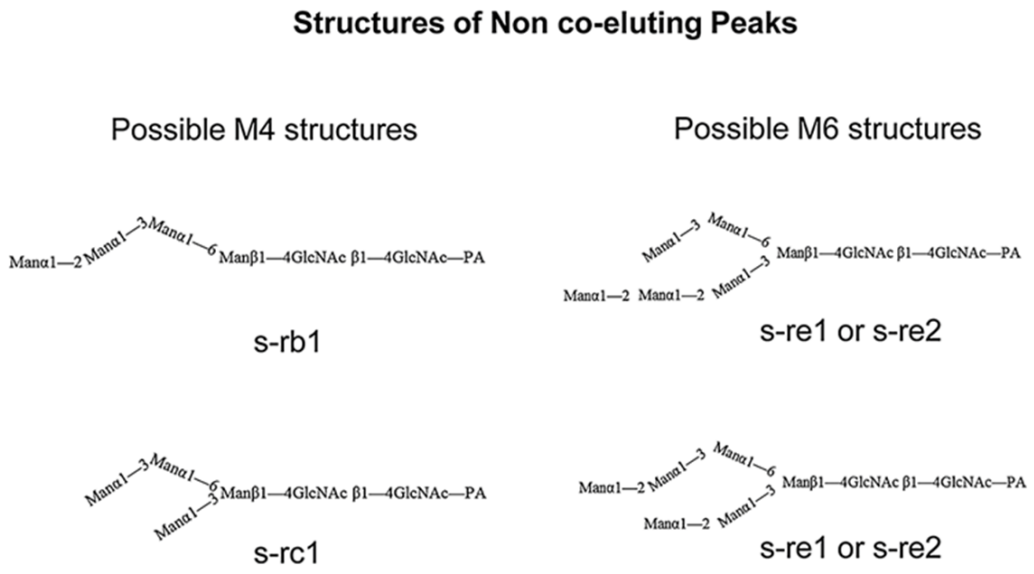

Figure 13. Proposed structures of the *N*-linked glycans peaks not co-eluting with standard PA-glycans.

Basidiomycetous yeast strains such as *C. neoformans var. neoformans* JEC21, *C. neoformans var. grubii* H99, *C. gattii* WM276 and *Rhodotorula turoloides* CECT1137 have putative mannosidases respectively annotated as CNA06750, CNAG_00696, CGB_A7550W and RHTO0_03e13080g belonging to the Glycosylhydrolases (GH) 38 family (Carbohydrate Active Enzyme database, http://www.cazy.org/). It is possible that certain α1-2/1-3 and/or α1-6 mannosidases belonging to the GH38 family could have cleaved the mannose residues resulting in the M4- and M6-sized PA-glycan structures of *S. paphiopedili*. On the basis of the structures of the M4- and M6-sized glycans, it can be presumed that these were possibly results of trimming by α mannosidases during *N*-linked glycan processing.

CONCLUSION

The glycan structures elucidated in this study provided an insight on the presence and abundance of high mannose neutral *N*-linked glycans delivered by *S. paphiopedili* which is a fundamental advance in comprehending the glycobiology of this yeast. In this manner, further examination of the structures and the biological roles of these *N*-linked glycans of *S. paphiopedili* are warranted. Lastly, *N*-linked glycan structural analysis of the other representative species from subphylum Ustilaginomycotina may provide further knowledge on their biological roles and the relationship of *N*-linked glycan structural diversity and yeast taxonomy.

Chapter 3

The Neutral *N*-linked Glycans of the Ustilaginomycete Yeasts

Pseudozyma antarctica and *Malassezia furfur*

INTRODUCTION

Yeasts are phylogenetically classified into two phyla, the Ascomycota with subphylum Saccharomycotina and Taphrinomycotina, and the Basidiomycota with subphylum Ustilaginomycotina, Agaricomycotina and Pucciniomycotina (Hibbett et al., 2007). In their life cycles, basidiomycetous yeasts possess both the yeast and mycelial stages. While other basidiomycetous yeasts are considered as animal pathogens such as the genera *Cryptococcus* and *Malassezia*, some are known to be plant pathogens, such as smuts and rusts. In addition, *Pseudozyma*, a basidiomycetous yeast, are commensals of different plant species, example of which is the *P. antarctica* frequently isolated in plant material such as leaves flowers and stem (Boekhout and Fell, 1998). On the other hand, *M. furfur*, a basidiomycetous yeast usually present on the skin surface of mammals, can potentially become pathogenic due to predisposing factors such as the health state of the host.

In spite of the fact that there are a few investigations on these species regarding their physiology, biology and biotechnological applications, their *N*-linked glycans have never been extensively examined in the past. This is with the exception of *M. furfur*, in which the linear β1-6 linked galactofuranose polysaccharides hefting around 30 residues were thought to be attached to the canonical *N*-linked core high mannose glycans interlinked by the yeast-type mannan polysaccharides (Shibata et al., 2009).

This study reports the neutral *N*-linked glycan structures of the basidiomycetous yeasts *P. antarctica* and *M. furfur*. High performance liquid chromatography (HPLC) and mass spectrometry (MS) analyses were performed following the extraction and processing of the neutral *N*-linked glycans from the three species. High mannose type glycans were observed in the neutral *N*-linked glycan fraction. The Manα1-2Manα1-6(Manα1-3)Manα1-6(Manα1-2Manα1-2Manα1-3)Manβ1-4GlcNAcβ1-4GlcNAc (M8A) glycan structure was found to be the most abundant type of glycan in the two species studied followed by Manα1-2Manα1-6(Manα1-2Manα1-3)Manα1-6(Manα1-2Manα1-2Manα1-3)Manβ1-4GlcNAcβ1-4GlcNAc (M9A) and Manα1-6(Manα1-3)Manα1-6(Manα1-3)Manβ1-4GlcNAcβ1-4GlcNAc (M5A) in *P. antarctica* and Manα1-2Manα1-6(Manα1-3)Manα1-6(Manα1-2Manα1-3)Manβ1-4GlcNAcβ1-4GlcNAc (M7A) was the second most abundant while M8A and M9A were ranked as third.

MATERIALS AND METHODS

P. antarctica (NBRC 10750) and *M. furfur* (IFM 48685) strains were obtained from the National Bioresource Research Center, NITE (Chiba, Japan) and the Medical Mycology Research Center of Chiba University (Chiba, Japan), respectively. *P. antarctica* was sub-cultured in 10 mL Yeast Extract Malt Extract Broth (YMB) for 48 h at 24˚C and afterward onto 100 mL of YMB with 10% glycerol. On the other hand, Yeast Peptone Dextrose (YPD) Broth supplemented with 1% olive oil was utilized to grow *M. furfur* at 30˚C. Following the 72 h of incubation, the yeast cells were collected by means of centrifugation at 6,000 rpm for 5 min. Glycoprotein extraction was then performed on the yeast pellet as described in chapter 2.

Glycan preparation by PA-tagging, HPLC, glycosidase digestions and mass spectrometric analyses were done under the same procedures discussed in chapter 2.

Monosaccharide component analysis was performed essentially as previously described (Hase et al., 1992). Peaks eluted later in NP-HPLC (peaks p-h and m-j) that might correspond to higher-sized high-mannose-type glycans were collected and lyophilized. Two milligrams of the lyophilized fraction were dissolved in 100 µL of 4 M hydrochloric acid at 100˚C for 3 h followed by repeated lyophilization. Re-*N*-acetylation was performed using 40 µL of pyridine: MeOH (1:9, v/v) and 10 µL of acetic anhydride at room temperature for 30 min followed by lyophilization.

The reducing ends of the released monosaccharides were fluorescently tagged by PA (Hase et al., 1978). The PA-monosaccharides (PA-Mono) were then lyophilized and dissolved in 100 µL

ultrapure water. Two µL of dissolved PA-Mono were isocratically eluted by HPLCgrade acetonitrile:0.8 M H_3BO_3-KOH at pH 9.0 (Solvent I, 1:9, v/v) using a TSKgel Sugar AXI column (4.6 mm x 150 mm; Tosoh, Tokyo) at 65˚C for 160 min.

RESULTS AND DISCUSSION

PA-glycans prepared from *P. antarctica* and *M. furfur* are composed of neutral *N*-linked glycans with varying sizes.

Figure 14 shows that the anion-exchange HPLC revealed peaks eluted within the elution times at which the acidic glycans of the standard human α1-acid glycoprotein which contains possibly one, two and three sialic acid residues are also eluted (Fournier et al., 2000). The structural complexity of glycans of some yeast may be brought about by acidic groups such as pyruvates and phosphates (Gemmill an Trimble, 1999). The neutral PA-glycan fractions were further separated in NP-HPLC, as shown in Figure 15. Well-separated $Man_{3\text{-}9}GlcNAc_2$PA-sized glycans peaks were collected, freeze-dried and dissolved for RP-HPLC analysis.

α-linked mannoses are attached to the non-reducing end of the *N*-linked glycans.

Jack bean α-mannosidase can hydrolyze the α1-2/3/6 Man linkages in the non-reducing terminal of the glycans (Li, 1967; Snaith and Levvy, 1968). It was used to affirm if the peaks contain α-linked Man residues at the non-reducing end. *P. antarctica* and *M. furfur* PA-glycan peaks eluted from the standard $Man_3GlcNAc_2$-PA position were digested resulting in a $Man_1GlcNAc_2$-PA (M1-PA) glycan as examined using NP-HPLC (Figure 15). To determine the elution position of the M1-PA glycan resultant peak, digested M9A-PA glycan standard was used. In light of the elution of peaks at the M1-PA glycan position, it can be surmised that α-linked Man residues are observed at the non-reducing terminal of the neutral PA-glycans.

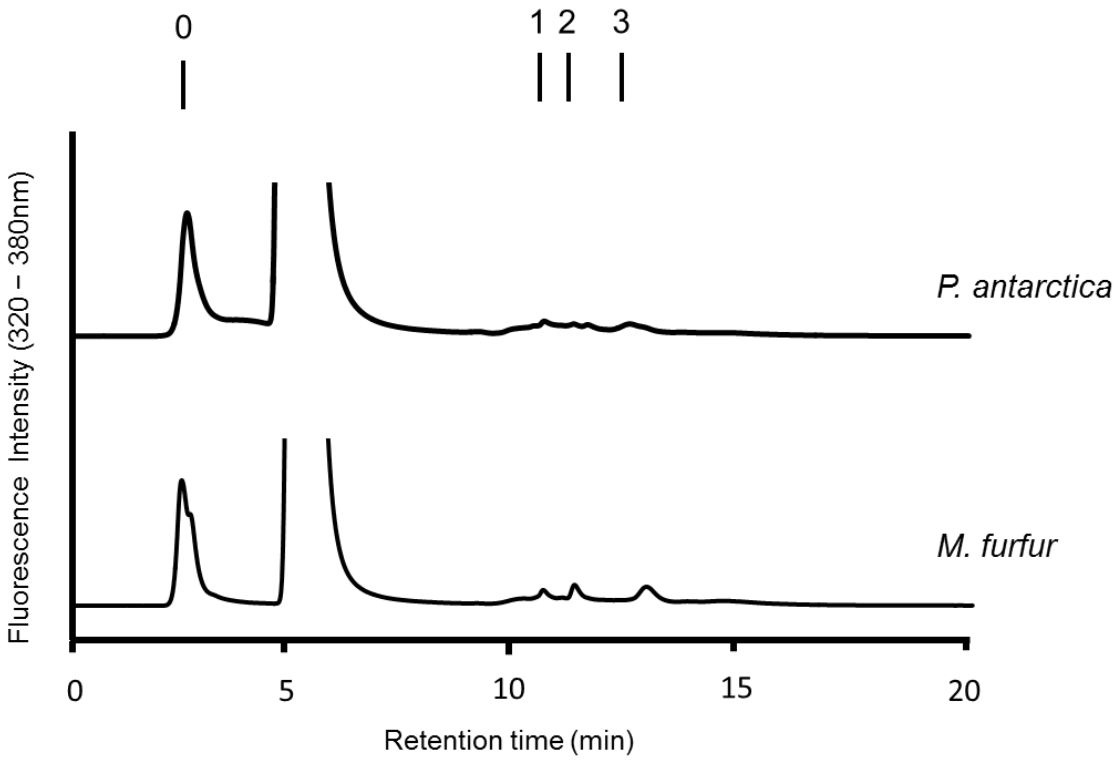

Figure 14. Anion-exchange HPLC (at 320 nm emission and 380 nm detection wavelengths) of PA-glycans from *P. antarctica* and *M. furfur*. PA-glycans from human *α*1-acid glycoprotein were used as the standard. The numbers and lines show the elution positions of standard PA-glycans containing zero to three sialic acid residues.

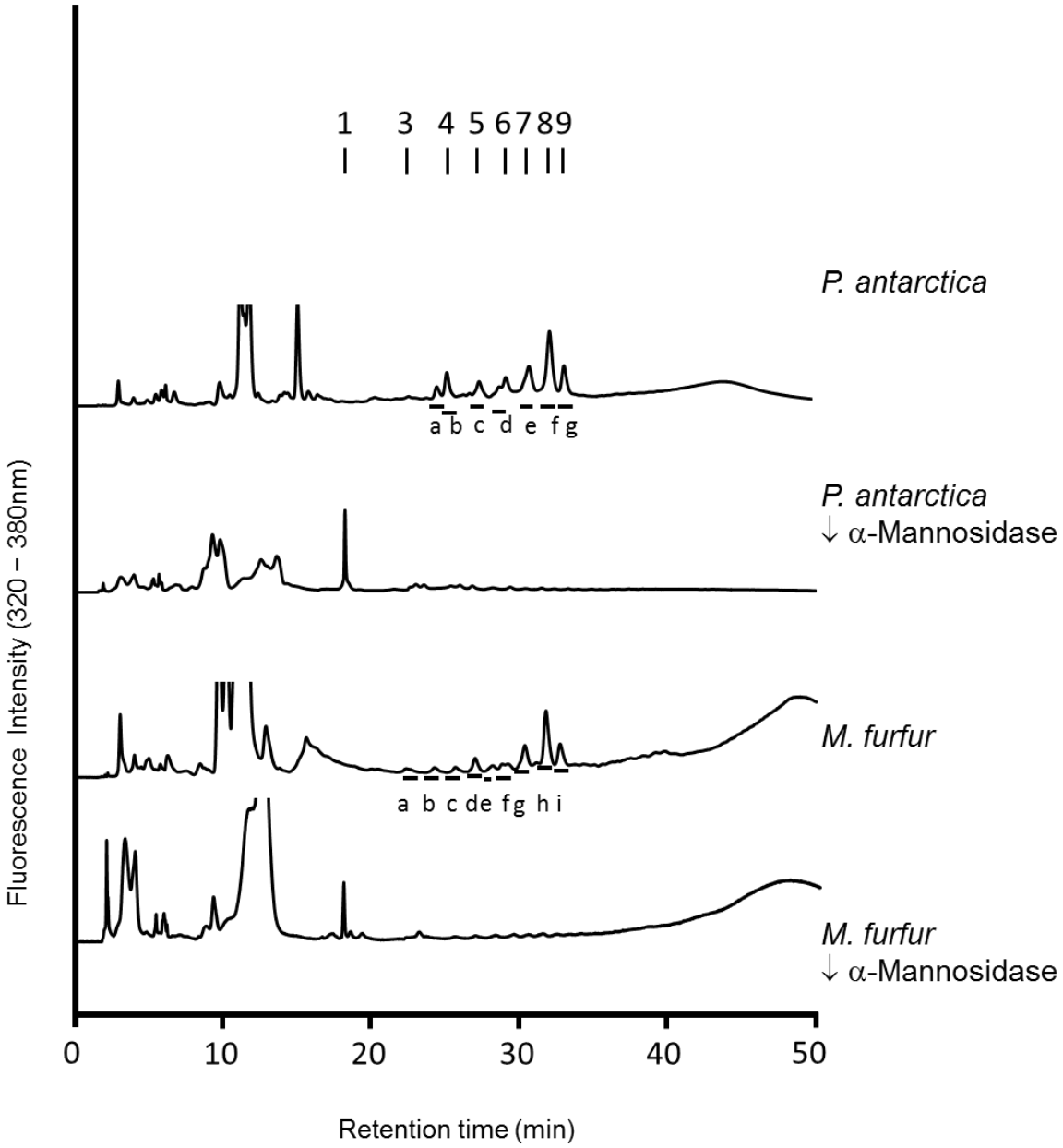

Figure 15. Normal-phase HPLC (at 320 nm emission and 380 nm detection wavelengths) of neutral PA-glycans. Neutral PA-glycans from anion-exchange chromatography were separated by normal-phase (NP) HPLC. Peaks eluting closely to standard $Man_{3–9}GlcNAc_2$-PA glycans were collected, labelled and lyophilized for further analysis. The numbers (1–9) on the chromatogram indicate the elution positions of standard M1-, M3-, M4-, M5-, M6-, M7-, M8- and M9-PA glycans. Jack bean *α*-mannosidase-digested peaks are also shown alongside the undigested sample.

The collected seven PA-glycan peaks of *P. antarctica* were designated as p-a, p-b, p-c, p-d, p-e, p-f and p-g, while the nine peaks of *M. furfur* were assigned as m-a, m-b, m-c, m-d, m-e, m-f, m-g, m-h and m-i. All of these peaks were eluted at positions close to those of the standard $Man_{3\text{-}9}GlcNAc_2$-PA glycans. Furthermore, peaks which were eluted later in the chromatograph may correspond to other higher molecular weight high mannose type glycans.

Isomeric forms of the isolated PA-glycan peaks were detected using RP-HPLC.

RP-HPLC were performed on the NP-HPLC-collected PA-glycans to separate and possibly distinguish different isomeric forms co-eluting with the standard PA-glycan isoforms. Some of the NP-HPLC peaks of *P. antarctica* and *M. furfur* are made up of various isomeric forms as presented by chromatogram peaks named accordingly in Figures 16 and 17. Based on co-elution with standard PA-glycans in both NP-HPLC and RP-HPLC, the structures of these abundant glycans were designated. It was observed in both NP-HPLC and RP-HPLC chromatograms that the presence of particular isomeric forms and their relative amounts differ among the species studied. In *P. antarctica*, the most abundant PA-glycan observed was M8A glycan (32%), followed by M9A (14%), then M5A glycan (11%). In the case of *M. furfur*, M8A was also found to be the most abundant at 25%, followed by M7A (16%), then M8B (15%) glycans. Interestingly, the M8A glycan structure was observed to be the major neutral PA-glycan for both *P. antarctica* and *M. furfur*. Some peaks that did not co-elute with standard PA-glycans were subjected to another glycosidase digestion and mass spectrometry analyses to confirm their composition and presumptive structures. Figure 18 shows the standard PA-glycans used in this study and their predicted structures.

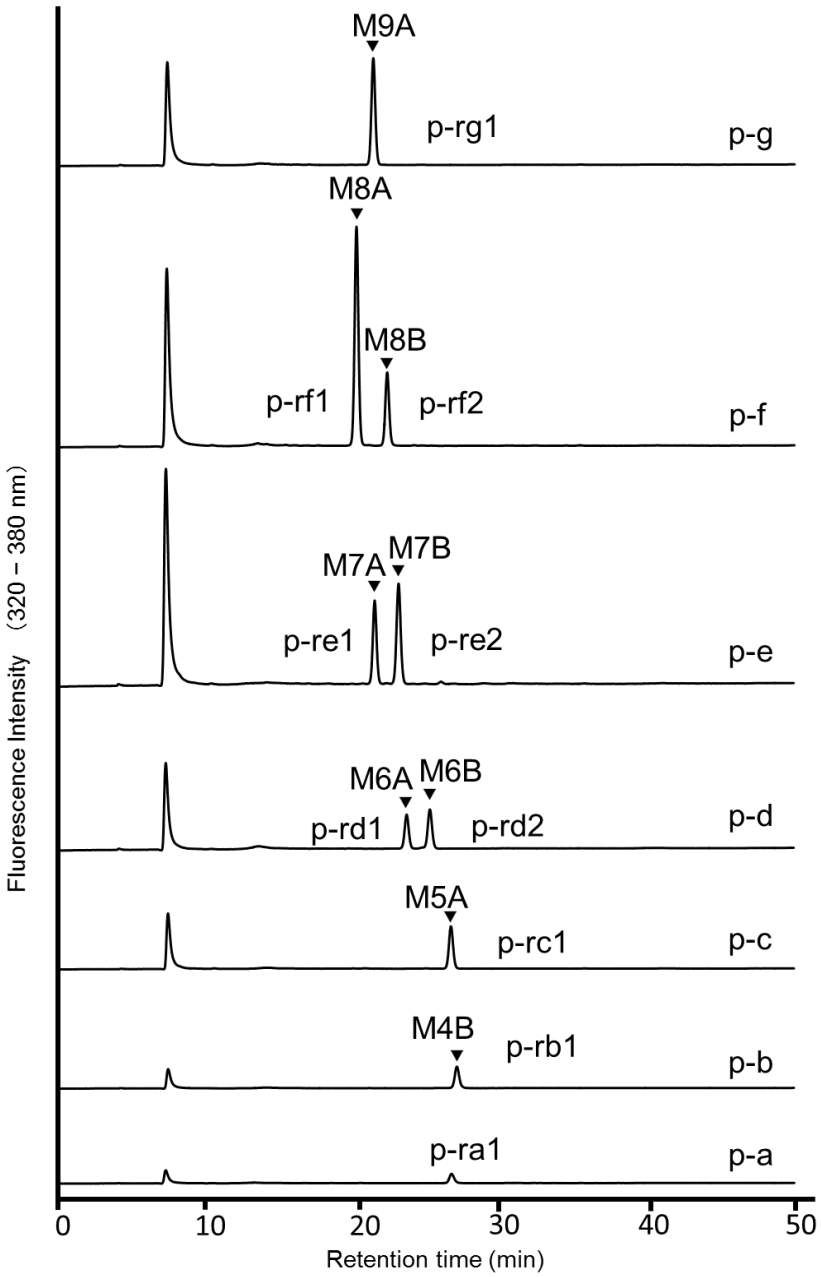

Figure 16. RP-HPLC at 320 nm emission and 380 nm detection of peaks p-a to p-g. Peaks p-a to p-g isolated from NP-HPLC were further separated by RP-HPLC. The arrowheads in the chromatograms show the elution positions of standard PA-glycans.

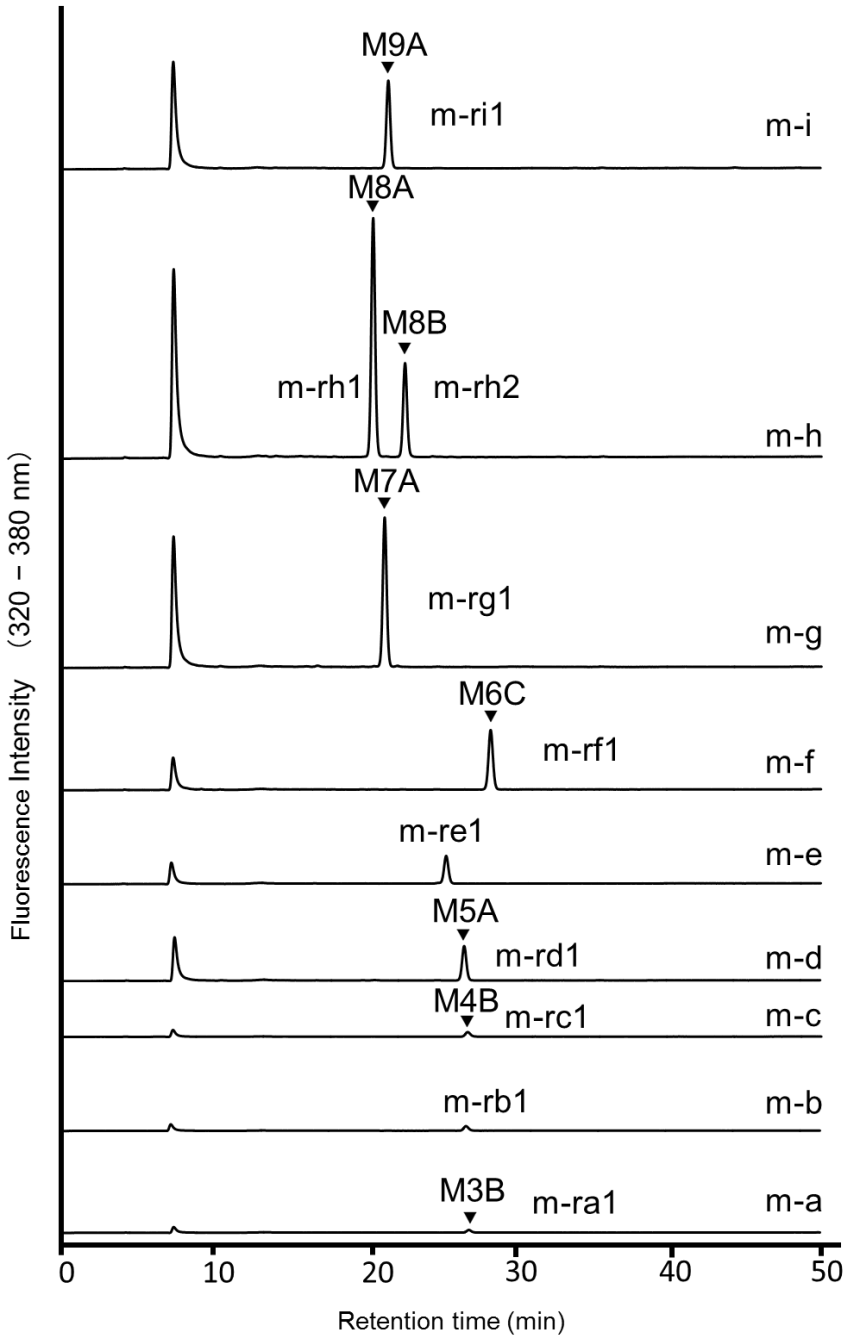

Figure 17. RP-HPLC (at 320 nm emission and 380 nm detection wavelengths) of peaks m-a to m-i. Peaks m-a to m-i isolated from NP-HPLC were further separated by RP-HPLC. The arrowheads in the chromatograms show the elution positions of standard PA-glycans.

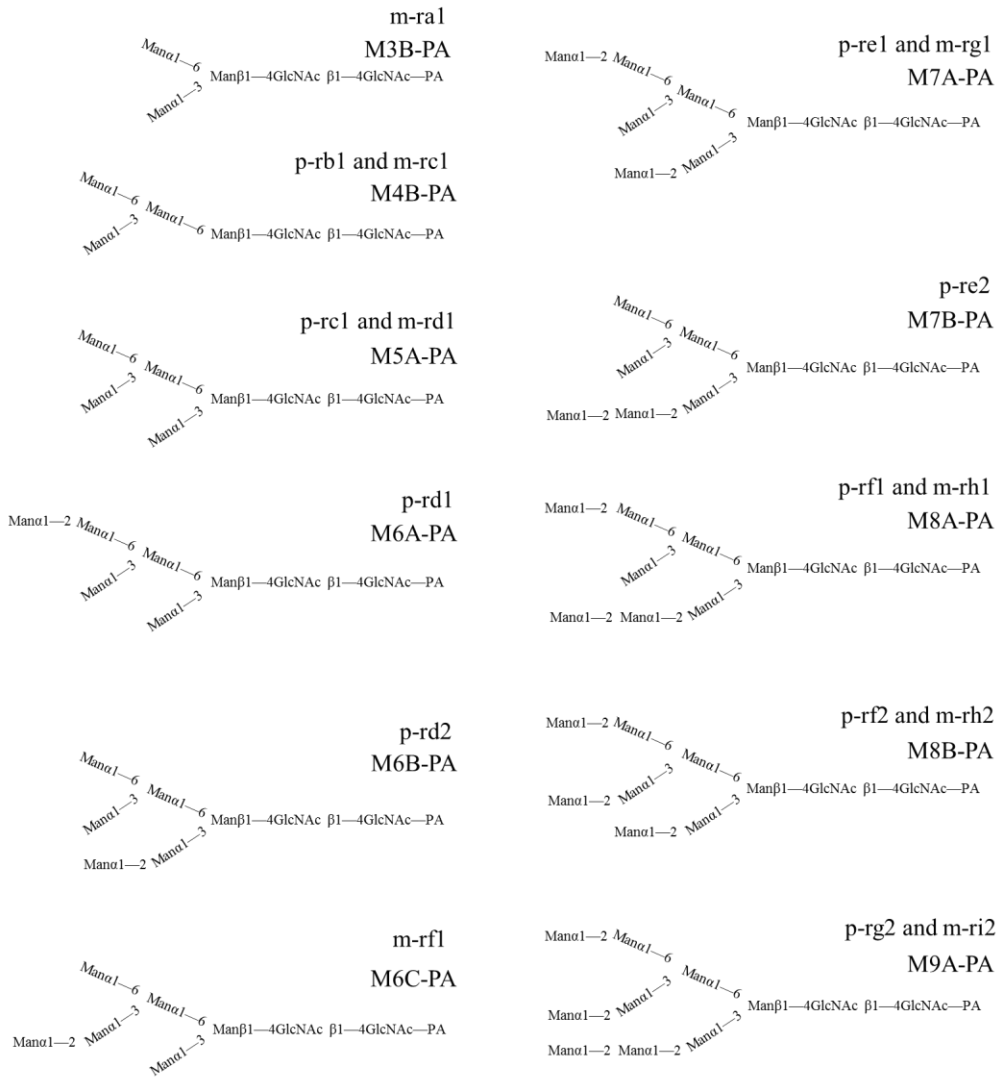

Figure 18. The structure of standard PA-glycans used in this study and the peaks that co-eluted in NP-HPLC and RP-HPLC.

Glycosidase digestion and mass spectrometry analyses of peaks p-ra1, m-rb1 and m-re1 which did not co-elute with standard PA-glycans revealed other possible glycan structures

While m-re1 might be identified as M6 glycan isomer other than M6A, M6B or M6C, peaks p-ra1 and m-rb1 co-eluted with each other in RP-HPLC and did not co-elute with standard PA-glycans could be distinguished as M4 glycan isomer other than M4B. To determine the manner of mannoses' linkages, the peaks were digested with α1-2 mannosidase, then with α1-6 mannosidase or α1-2/1-3 mannosidase in a successive manner. Peaks p-ra1, m-rb1 and m-re1 glycans were subjected to digestion with α1-2 mannosidase and detected using NP-HPLC. Peaks p-ra1 and m-rb1 each yielded a M3-sized peaks (p-ra1a and m-rb1a) after digestion with α1-2 mannosidase which suggests the presence of one α1-2 linked mannose. Peaks p-ra1a and m-rb1a were collected and separately subjected to digestion with α1-2/1-3 mannosidase, both yielded an M2-sized peak indicating the presence of one α1-3 linked mannose. Then, the peaks were digested with α1-6 mannosidase, however, the digestion suggests that the peaks were not susceptible indicating the possibility that they are consist of an α1-6 mannose to which another α1-3 mannose is connected (Manα1-3Manα1-6Manβ1-4GlcNAcβ1-4GlcNAc-PA). The α1-6 mannosidase enzyme was successful in digesting the M4B-PA using the same enzymatic conditions. In addition, the m-re1 peak produced an M4-sized peak (m-re1a) after digestion with α1-2 mannosidase indicates the presence of two α1-2 linked mannoses. The m-re1a peak yielded an M2-sized glycan after digestion with α1-2/1-3 mannosidase which indicates the presence of two α1-3 linked mannoses but it was not susceptible to α1-6 mannosidase. The digestion profiles are presented in Figure 19.

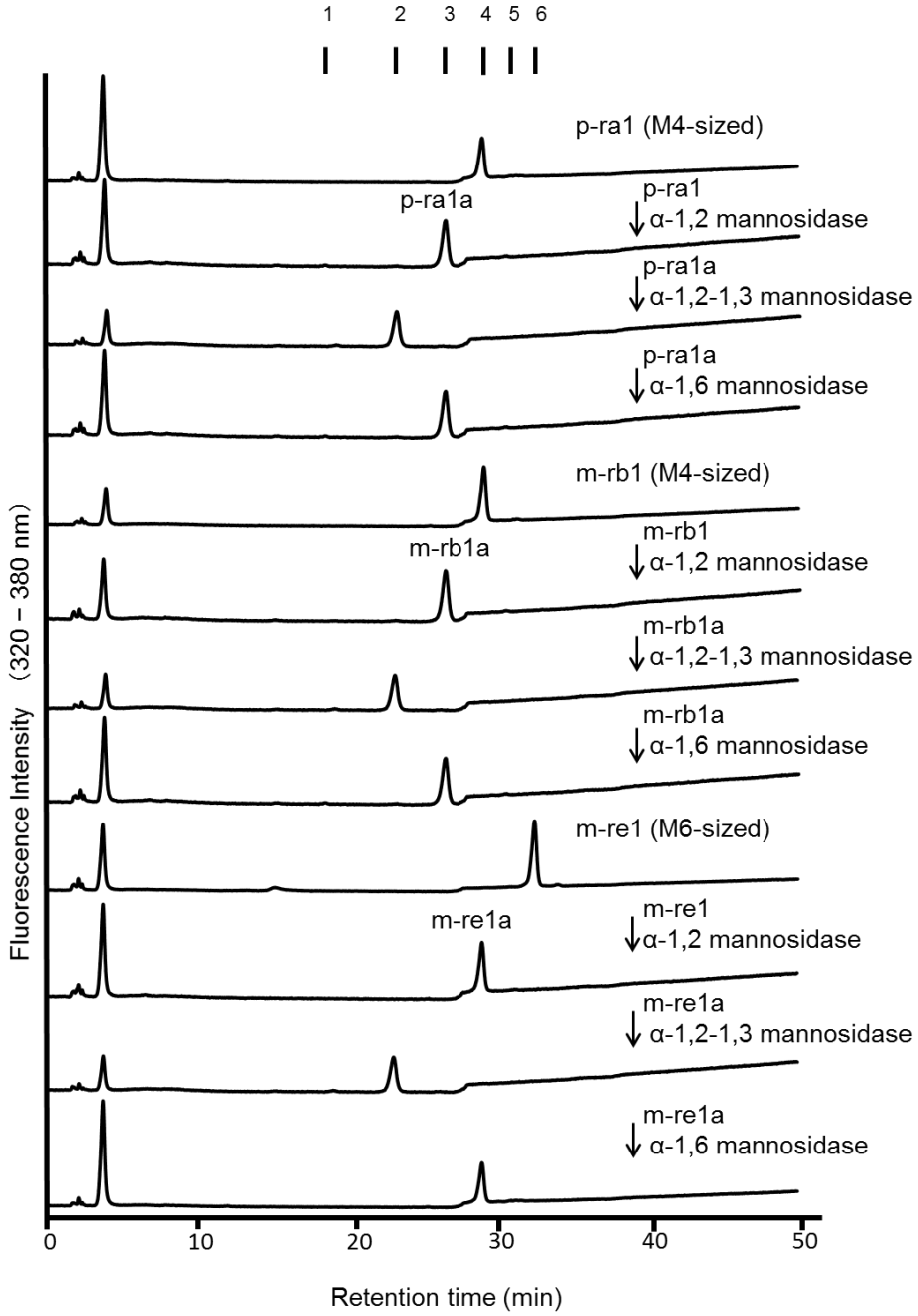

Figure 19. Sequential mannosidase digestion profile of unknown M4 (p-ra1 and m-rb1) and M6-sized (m-re1) glycan. The numbers (1–6) on the NP-HPLC (at 320 nm emission and 380 nm detection wavelengths) chromatogram indicate the elution positions of standard M1-, M2-, M3-, M4-, M5-, and M6-PA glycans.

To confirm the composition of the individual RP-HPLC-isolated peaks corresponding to the isomeric forms of the detected high mannose type glycans, LC-MS/MS analysis was performed. Figure 20 presents the LC-MS/MS analyses of M4-sized glycans (peak p-ra1 and peak m-rb1) and an M6-sized glycan (peak m-re1), which did not co-elute with standard PA-glycans, showing the corresponding fragmentation patterns. Fragmentation patterns and *m/z* were used to determine the composition of the peaks. The full length of the presumptive $Man_4GlcNac_2$-PA-glycan peaks (p-ra1 and peak m-rb1) yielded *m/z* of 1152.0 $[M+H]^+$ and 1152.2 $[M+H]^+$ respectively, with each succeeding fragment ion loss corresponding to one hexose residue while the *m/z* of 503.2 relates to the GlcNAcβ1-4GlcNAc-PA (Figure 20A and 20B). In addition, the full length of presumptive $Man_6GlcNAc_2$-PA glycan (peak m-re1) yielded an *m/z* of 1476.3 $[M+H]^+$ in which each preceding generated fragment ion corresponds to a loss of a hexose residue with *m/z* of 503.3 analogous to the GlcNAcβ1-4GlcNAc-PA (Figure 20C). Considering the results of the mannosidase digestion, HPLC and mass spectrometry analyses of the PA-glycan samples, it can be concluded that the *N*-linked glycans of the two species are of the high mannose type. Moreover, the size range of the *N*-linked glycans was $Man_{4\text{-}9}GlcNAc_2$ in *P. antarctica* and $Man_{3\text{-}9}GlcNAc_2$ in *M. furfur*. Tables 3 and 4 summarize the composition, structure designation and percentage of the various peaks detected. P-ra1, m-rb1 and m-re1, peaks that did not co-elute perfectly with standard PA-glycans in RP-HPLC but whose compositions were confirmed to have hexoses in MS, may have been considered as other possible isomeric forms of the standard glycans. Figure 21 shows the proposed structures for these non-co-eluting peaks based on glycosidase digestions and mass spectrometry.

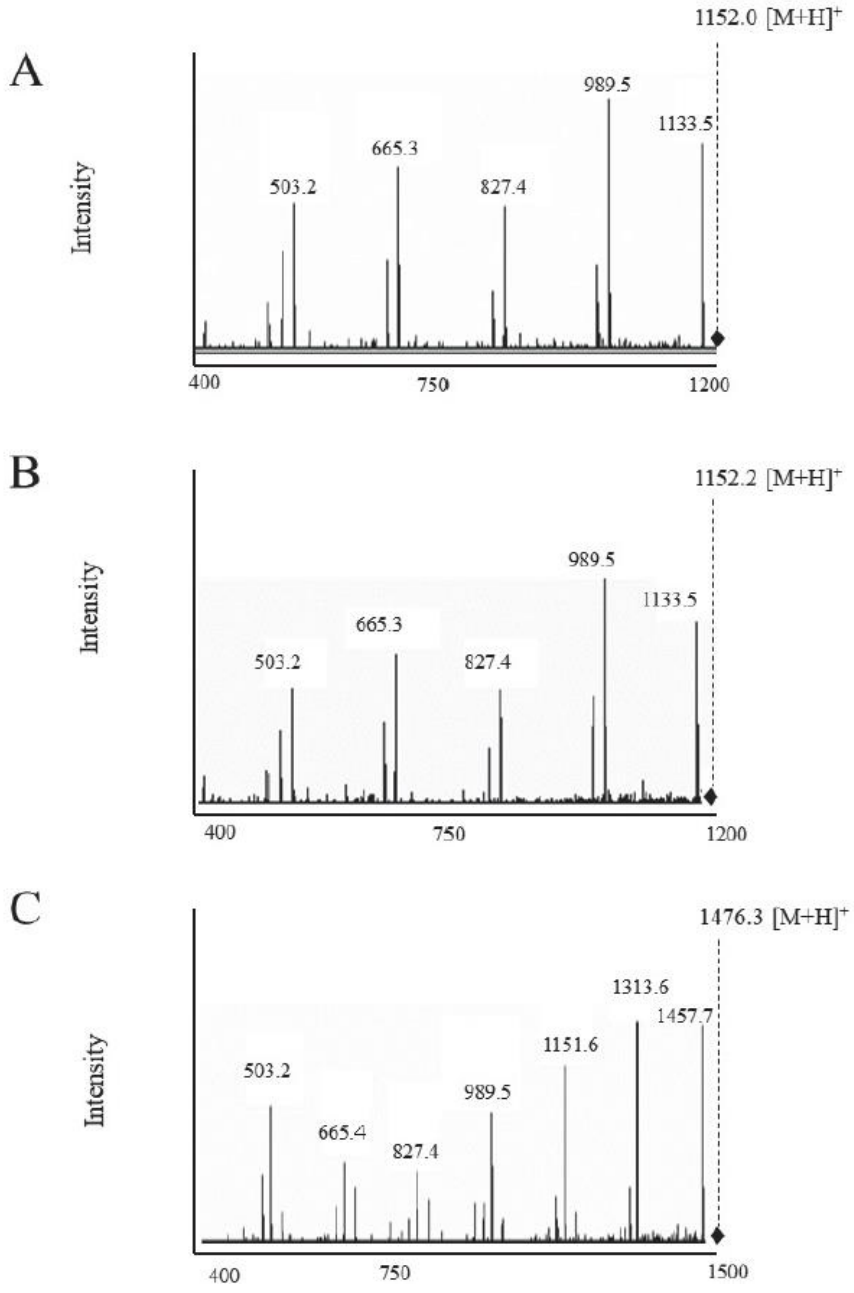

Figure 20. Mass spectrometric analysis of the peaks that did not co-elute with the standards in HPLC. Mass spectrometric data show that fragmentation results in one loss of hexose. (A) Peak p-ra1; (B) peak m-rb1; (C) peak m-re1. The rhombus (♦) indicates the *m/z* of the precursor ion. $[M + H]^+$ adduct ions were detected.

Table 3. Peak designation, confirmed identity, elution time in NP-HPLC and RP-HPLC, *m/z* and percentage quantity of neutral *N*-linked glycans of *P. antarctica.*

Peak	Composition	Elution Time (min) (NP-HPLC)	Elution Time (min) (RP-HPLC)	*m/z*	Identity	Abundance%
p-ra1	$Hex_4GlcNAc_2$	24.5	26.9	1152.0	M4*	3.9
p-rb1	$Hex_4GlcNAc_2$	25.0	27.0	1152.1	M4B	7.1
p-rc1	$Hex_5GlcNAc_2$	28.0	26.4	1314.4	M5A	11
p-rd1	$Hex_6GlcNAc_2$	29.3	23.7	1476.5	M6A	5.5
p-rd2	$Hex_6GlcNAc_2$	29.3	25.2	1476.5	M6B	4.9
p-re1	$Hex_7GlcNAc_2$	30.3	21.5	1638.4	M7A	8.1
p-re2	$Hex_7GlcNAc_2$	30.3	23.1	1637.9	M7B	8.0
p-rf1	$Hex_8GlcNAc_2$	31.5	20.2	1800.9	M8A	32
p-rf2	$Hex_8GlcNAc_2$	31.5	22.3	1800.7	M8B	5.5
p-rg1	$Hex_9GlcNAc_2$	32.5	21.2	1962.7	M9A	14

***** Possible isomer other than M4B

Table 4. Peak designation, confirmed identity, elution time in NP-HPLC and RP-HPLC, *m/z* and percentage quantity of neutral *N*-linked glycans of *M. furfur*.

Peak	Composition	Elution Time (min) (NP-HPLC)	Elution Time (min) (RP-HPLC)	*m/z*	Identity	Abundance%
m-ra1	$Hex_3GlcNAc_2$	22.5	26.8	990.1	M3B	3.0
m-rb1	$Hex_4GlcNAc_2$	24.5	26.9	1152.2	M4*	3.0
m-rc1	$Hex_4GlcNAc_2$	26.2	27.0	1152.0	M4B	3.2
m-rd1	$Hex_5GlcNAc_2$	28.0	26.8	1314.4	M5A	7.8
m-re1	$Hex_6GlcNAc_2$	28.5	25.0	1476.3	M6**	5.2
m-rf1	$Hex_6GlcNAc_2$	29.3	28.2	1476.9	M6C	6.8
m-rg1	$Hex_7GlcNAc_2$	30.3	21.5	1638.8	M7A	16
m-rh1	$Hex_8GlcNAc_2$	31.5	20.2	1800.5	M8A	25
m-rh2	$Hex_8GlcNAc_2$	31.5	22.3	1800.7	M8B	15
m-ri1	$Hex_9GlcNAc_2$	32.5	21.2	1962.7	M9A	15

***** Possible isomer other than M4B

** Possible isomers other than M6A or M6B

Possible M4 structure

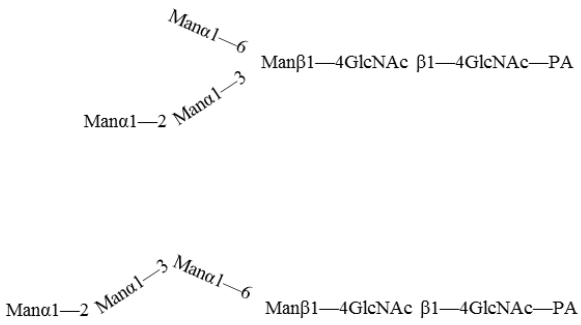

Possible M6 structure

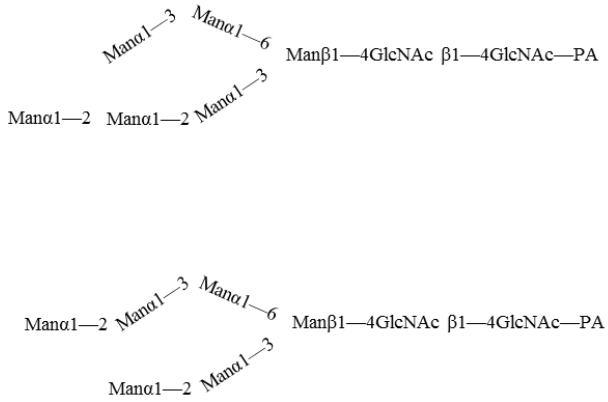

Figure 21. Some other possible isomeric structures of unique M4 and M6 glycan structures.

Based on the structures of the M4- and M6-sized glycans, it can be hypothesized that these were possible results of *N*-linked glycan processing by α mannosidases. Putative mannosidases respectively annotated as CNA06750, CNAG_00696, CGB_A7550W and RHTO0_03e13080g which belong to the Glycosylhydrolases (GH) 38 family are present in other basidiomycetous yeast strains such as *C. neoformans var. neoformans* JEC21, *C. neoformans var. grubii* H99, *C. gattii* WM276 and *Rhodotorula turoloides* CECT1137 (Carbohydrate Active Enzyme database, http://www.cazy.org/: Lombard et al., 2014). Therefore, certain α1-2/1-3 and/or α1-6 mannosidases that belongs to the GH38 family were responsible for cleaving mannose residues which resulted in the M4- and M6-sized PA-glycan structures of both *P. antarctica* and *M. furfur*.

Basic Local Alignment Search Tool (BLAST) analysis revealed the presence of putative mannosidase genes and proteins, some of which theoretically belong to GH 38, 47 and 92 families, within other strains of *P. antarctica* namely JCM 10317 and T-34 whose draft genome and full genome sequences have been respectively analyzed (Boratyn et al., 2013; Morita et al., 2013, Saika et al., 2014). These proteins were annotated in the NCBI (National Center for Biotechnology Information) database as XP_014659398.1, XP_014654165.1, and XP_014658277.1. These putative mannosidase proteins and the genes encoding them are currently the targets for further characterization and analysis.

Galactose residues were detected in the fraction corresponding to higher-sized *N*-linked glycans

β1-6 galactofuranose-containing galactomannan antigens was previously reported present in the cell wall of *M. furfur* (NBRC 0656) (Shibata et al., 2009). Nuclear Magnetic Resonance (NMR) and antibody reactivity were used by Shibata et al. to prepare and scrutinize the cell wall polysaccharides. They also suggested that the galactofuranose residues are present and have postulated, and are bound to the non-reducing end of the typical yeast type mannan structure (galactomannan) in *N*-linked glycans. However, the direct link of β1-6 galactofuranose-containing galactomannan to the *N*-linked glycans was unknown. To verify this claim, the eluted peak of *M. furfur* in NP-HPLC was collected, lyophilized and subjected to monosaccharide component analysis. Upon acid hydrolysis and PA-tagging, galactofuranose can then be detectable as Gal-PA since the 2-aminopyridine coupled with reduction results in the modification of the furanose. Gal-PA is included in the peaks of the identifiable monosaccharides detected and presented in Figure 22. Through this, it can be assumed that galactofuranose residues might also be present in the putative higher-sized glycan fraction in NP-HPLC and in the putative higher-sized neutral *N*-linked glycans and/or possible glucans that have co-eluted together in the neutral fraction of DEAE-HPLC analysis. Hence, the detection of a Gal-PA peak supports the previous report by Shibata et al. on the presence of galactofuranose residues on the cell wall galactomannan antigen of *M. furfur*.

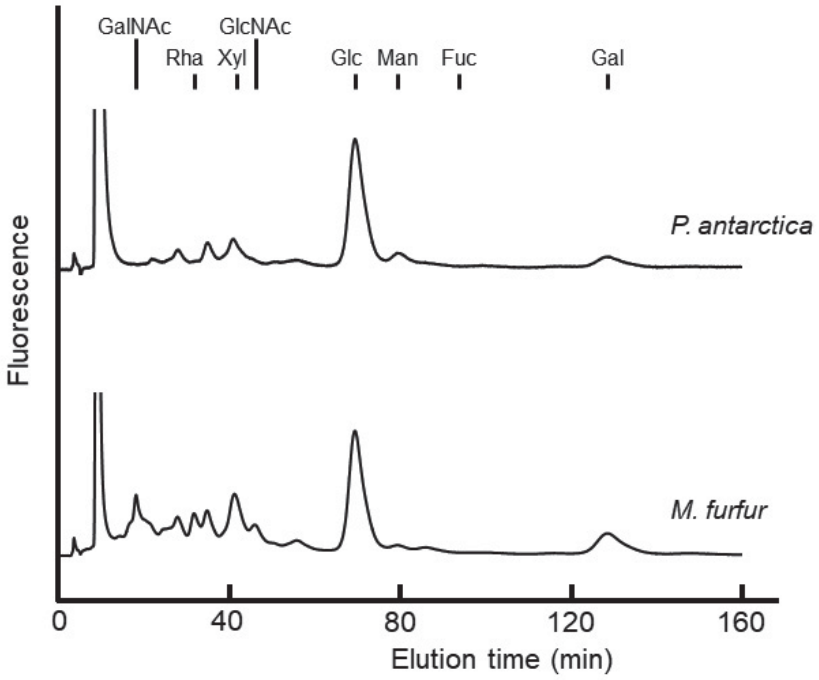

Figure 22. Monosaccharide component analysis showing detection of galactose peaks in *M. furfur*.

CONCLUSION

This elucidation of the various neutral *N*-linked glycans initiated a necessary step towards the understanding of the glycosylation of the biotechnologically important *P. antarctica* and the medically relevant *M. furfur*. Although the specific biological roles of these glycans are not yet elucidated, it can be taken into consideration that the observed range of neutral *N*-linked glycans in *P. antarctica* (order Ustilaginales) and *M. furfur* (order *Malassezia*les) corresponds with the range previously established in *S. paphiopedili* (order Microstomatales). Remarkably, M8A was found to be the most abundant structure detected in the high mannose *N*-linked glycan fraction in the 3 representative yeasts species of the three orders under the subphylum Basidiomycota.

Chapter 4

Discussion and Conclusion

Prospects on Glycan Stucture Elucidation

Chapters 2 and 3 dealt with the detectable neutral *N*-linked glycan structures that were present in glycoproteins of the *S. paphiopedili, P. antarctica* and *M. furfur*. Interestingly, the single common dominant *N*-linked glycan structure in these three species was the M8A glycan. Table 5 shows the 3 most dominant structures and their corresponding proportions. This may be explained by the highly similar glycan structures in these species which may support the notion that closely related organisms share the same characteristics. This discovery also may provide an initial postulation that Ustilaginomycete yeast *N*-linked glycans are shorter and simpler than their Agaricomycetous yeasts counterparts, as discussed earlier, which has bigger and more extensive *N*-linked glycan moieties. The differentiation in dominant *N*-linked glycan size and complexity is important since the core glycan structure of both groups is typical of eukaryotic core *N*-linked glycan.

This conservativeness of the core glycan has long been proven since the early steps of the *N*-linked glycosylation pathway have been long regarded as a highly conservative process especially in the eukaryotes. However, a closer look at the minute details and nuances in the glycosylation processing of taxonomically placed species may help further the understanding of the similarities or differences that may either be used to group them together or separate them apart. The discovery of unique glycan structures opens up a new avenue for research exploration as these unique glycans may have been results of a number of novel glcosylation-related enzymes and may have novel biological functions. The abundance of the M8A structure raises insights as to the possible post translational processing involved in these 3 species that led to the trimming of the glycans.

Table 5. Summary of the 3 most common dominant structues in *S. paphiopedili, P. antarctica and M. furfur*.

Species	*M. furfur*	*S. paphiopedili*	*S. paphiopedili*
1st Dominant Structure	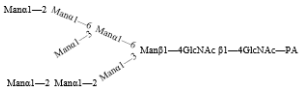 M8A (25%)	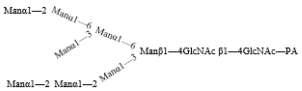 M8A (24%)	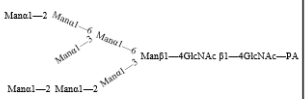 M8A (32%)
2nd Dominant Structure	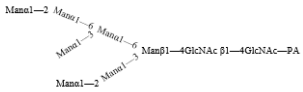 M7A (16%)	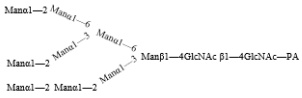 M9A (15%)	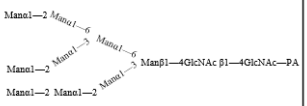 M9A (14%)
3rd Dominant Structure	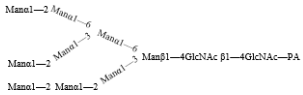 M9A (15%)	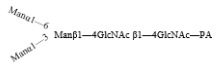 M3B (15%)	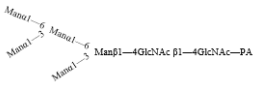 M5A (11%)

Putative α mannosidases may have caused the dominance of smaller high mannose glycans, and therefore should be the targets of future investigations. *N*-linked glycosylation occurring in ER have been demonstrated to be conserved among eukaryotic lineages. It is believed that diversity and uniqueness of *N*-linked glycosylation is a result of the enzymes, including mannosidases, in the pathways of the Golgi (Wang et al., 2017). On the average, 27% of the *N*-linked glycans of the 3 species are of the M8A structure. Meanwhile, the M9A structure has an average of almost 15% in abundance, making it the second most common abundant structure. The loss of 1 mannose residue may have been a result of another trimming mechanism brought about by an α 1-2 mannosidase that cleaves a mannose attached to middle mannose branch. This enzyme maybe a key enzyme that results in the abundance of the M8A from the M9A structure. The abundance of M3A (core glycan structure) in *M. furfur* is also intriguing in the sense that the a high relatively high proportion (15%) is cleaved to only 3 mannoses possibly suggesting a very efficient trimming mechanism.

Furthermore, the determination in chapter 2 that the best combination of extraction and release protocol is that of citrate extraction and hydrazine release is a major contribution to body of scientific knowledge since it would help streamline future work on the protocols for extraction of *N*-linked glycans in basidiomycetous yeasts. Moreover, the detection of galactose moieties in *N*-linked glycan fractions of *M. furfur* in chapter 3 is also a major addition to the body of scientific knowledge with the identification of the attachment of galactose to neutral *N*-linked glycan moieties, which was previously unknown. The presence of β1-6 galactofuranose-containing

galactomannan antigens in the cell wall of *M. furfur* NBRC 0656 was previously reported by Shibata et al. (2009). In their investigation, cell wall polysaccharides were resolved to be the β1-6 galactofuranose-containing yeast-type mannan structure made out of a α1-6 linked Man backbone linked with α1-2 linked Man residues based on the analyses they conducted such as nuclear magnetic resonance (NMR) and antibody reactivity analyses. As in chapter 3, the detection of a Gal-PA peak affirms the previous inference of Shibata et al. that galactofuranose residues exist on the *N*-linked glycans in *M. furfur*.

Prospects on Fungal Classification

The primary goal for fungal taxonomy is the establishment of a natural classification. Polyphasic approaches are being considered by many scientists as more reliable criteria for taxonomic studies. Polyphasic taxonomy includes morphological, physiological, ecological molecular and chemical approaches in resolving issues of classification and taxonomy. As early as the 1960s, the presence of certain sugars on fungal cell walls is regarded as a determining factor in classification such as in the case of D-galactose and D-galactosamine for Ascomycetes, L-fucose for Mucorales and Basidiomycetes, D-glucosamine in Mucorales, among others (Bartnicki-Garcia, 1968).The sugar composition of the fungal cell walls had been traditionally as a criterion for the taxonomy and systematics of filamentous fungi (Bartnicki-Garcia 1968, Leal et al., 1997, Leal and Bernabe 1998), yeasts (Gorin and Spencer, 1970) and lichen mycobionts (Teixeira et al., 1995). Numerous studies have shown differences in the structure and composition of the cell wall of fungi which have been used in the definition of fungal taxa. The walls of yeast cells that have

been subjected to hydrolysis yield substantial amounts of glucose and mannose, but species differ in the presence or absence of smaller amounts of other polysaccharides (fucose, galactose, rhamnose, and xylose). Bartnicki-Garcia (1987) has reviewed the biochemical and physiological characteristics of the cell wall components which have been used to delimit high taxa.

A multitude of researches on fungal classification have been published all over the world. Fungal classification had been very dynamic largely due to the impact of the influx of new approaches and techniques which can be used in classification. This has been revolutionized by the development of more advanced techniques in fungal cell wall chemotaxonomic and phylogenetic analyses. However, the correlation between the appearance or the loss of a polysaccharide over time and the corresponding fungal taxonomy, is considered to not be absolute (Latgé and Calderone, 2005). Fungal morphotypes in the same species exhibit differences in sugars present. This shows a tight regulation of cell wall synthesis throughout the cell cycle (Latge, 2007). With the ever-changing nature of the fungal cell wall and the development of methods to analyze them, lies the depth and dynamism of the fungal classification.

This higher level classification by Tedersoo et al. currently upgrades the higher order classification of Hibbett et al. (2007) by virtue of the compilation and analysis of more current systematic and evolutionary data. The Hibbett classification is similar to the one proposed by Bauer et al. (2006). The study of Tedersoo et al. (2018) outlined the currently accepted higher level fungal classification scheme which is now being adapted all over the world. In the case of phylum Ascomycota, there were four new classes resolved under subphylum Pezizomycotina namely

Collemopsidiomycetes, Coniocybomycetes and Geoglossomycetes. On the other hand, there was one class resolved under subphylum Taphriniomycotina by the name Archeorhizomycetes. These were not previously present in the Hibbet classification (2007).

Basidiomycota has been divided to include four subphyla namely Agaricomycotina, Pucciniomycotina, Ustilaginomycotina and Wallemiomycotina. The most obvious change was the promotion of the *incertae cedis* (not belonging to any next higher taxon) class Wallemiomycetes into a subphylum now known as Wallemiomycotina. It is interesting to note that a number of taxa under the Hibbett classification had been included as *increate cedis* such as Wallemiomycetes and Entorrhizomycetes. In addition, the previously categorized *incertae cedis* order Malasseziales under subphylum Ustilaginomycotina is now considered a distinct class Malasseziomycetes. Order Malasseziales was traditionally found to be included in Ustilaginomycetes on the basis of protein-coding genes *rpb1, rpb2,* and *tef1* together with nuclear large sub-unit (LSU), small sub-unit (SSU) and 5.8S ribosomal genes but has been found to be included in the Exobasidiomycetes on the basis of nuclear ribosomal genes and/or *atp6* and beta-tubulin genes (Bauer et al., 2001; Begerow et al., 2007; Matheny et al., 2007; Weis et al., 2004, as cited in Hibbett et al., 2007).

Molecular revolution in fungal taxonomy started in the 1990s with the advent of PCR-based analyses using ribosomal RNA genes (White et al., 1990). Since then, molecular phylogenetic analyses have placed Phylum Basidiomycota and the entire kingdom Fungi under scrutiny. Various groups of scientists have proposed a number of classification schemes and changes throughout the years. Moreover, a number of criteria for species identification which involve molecular and biochemical analyses have been used in recent years. The nucleotide

sequences of the domain 1 and domain 2 of the LSU of the 23S rRNA have been very useful in identifying up to the species level (Fell et al., 2000: Kurtzman, 2006). The internal transcribed spacer (ITS) regions have also been used to efficiently identify various yeasts species (Scorzetti et al., 2002).

The determination of the abundance of the M8A as the common most abundant (average of 27% in the 3 species) and the M9A (average of 15%) raises the possibility that these may be used a determining criteria in establishing ustilaginomycte taxonomy. This is parallel to the chemotaxonomic method of earlier classifications wherein the sugar composition of the cell wall was considered. Furthermore, the ratio of the neutral *N*-linked glycans produced at the specific conditions for growth and processing may probably be used as an addition character to establish unity in the high level classification. In juxtaposition, the presence as well as the ratio of the novel glycans discovered in the 3 species may probably be used in order to characterize the individual species. The remaining challenge for fungal taxonomy is the widening of the database of neutral *N*-linked glycan structures in order to fully appreciate and understand the usability of this chemical information to taxonomy. Reconciling the scheme of chemotaxonomy with current molecular phylogeny can be achieved if more information on the diversity of *N*-linked glycans in other basidiomycetous yeasts will be databased. Figure 23 shows the distribution of the most abundant M8A structure in the 3 species as compared with the most abundant structures in the other subphyla. Additional representative species from the four classes under Ustilaginomycotina and other subphyla should be studied in order to understand the usability of the *N*-linked glycan as a character for determining ustilaginomycetous taxonomy and classification.

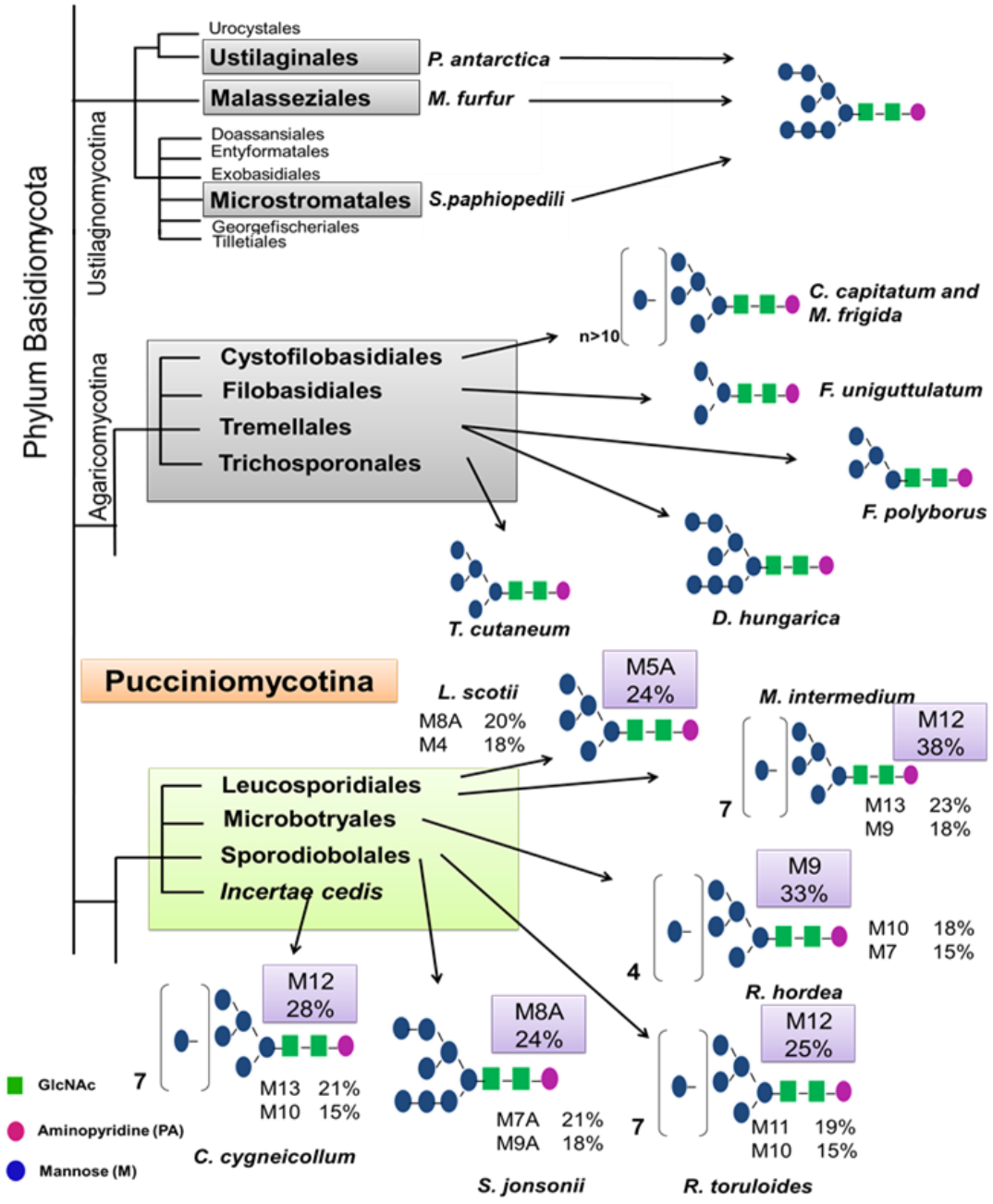

Figure 23. A diagrammatic representation of the most abundant *N*-linked glycan structures of different representative species in the Basidiomycota.

Prospects on Possible Biotechnological Applications

The importance of protein glycosylation for the biotech industry is highlighted by the fact that approximately 70% of therapeutic proteins approved or in pre-clinical studies, are glycoproteins. Knowing the glycan structures present is a necessary step in understanding that biological significance of such glycosylation. In the case of the smaller sized high mannose type glycans of the 3 species studied in this thesis, the potential to jumpstart the search for enzymes is highlighted. This also recognizes the tremendous biotechnological applications of these yeasts as being suitable alternatives to mammalian cell cultures in production of heterologous protein (Gerngrosss, 2004). *P. antarctica* had been observed to be an excellent producer recombinant proteins and mannosylerythritol lipids (MELs) which may have had a great biotechnological application as a biosurfactant, antitumor, cell-differentiation inducer, moisturizer and hair-repairer (Avis et al., 2005; Kitamoto et al., 1990; Kitamoto et al., 2002; Kitamoto et al., 2009). In addition, enzymes produced by *P. antarctica* have been utilized to degrade biodegradable polymers (Shinozaki et al., 2013). *P. antarctica* itself had been utilized as a host for high-level recombinant protein production of biodegradable plastic-degrading enzyme which plainly underscores the biotechnological potential of this yeast (Watanabe et al., 2016).

Glycobiotechnology uses new techniques to manuplate carbohydrates or related materials for the betterment of our lives; its development is intimately related to the progress of glycobiology. Complex molecules as applied into analytical and therapeutic studies resulted from the

development of “glycobiotechnology” as an interdisciplinary research field (Elling, 2007). Alongside DNA and proteins, sugar structures play an important role in cellular transport and communication processes. They are also part of the molecular control and regulation machinery making them of particular interest to biotechnologists. The pharmaceutical industry, as well as the food sector and material sciences, have realised the potential of sugar structures. Better analytical methods and a growing and deeper understanding of cellular mechanisms revealed that sugar structures had far more biological functions than previously thought. As a result, glycobiology has received greater attention in recent years. One example is to utilize carbohydrate recognition. Furthermore, the glycans natural glycoproteins or glycolipids can be modified or removed for the same purpose or be targeted as a means of treatment. Likewise, these glycoproteins can be used as potential treatments themselves. With this analysis of structures of carbohydrate chains are very important in understanding the biological recognition of carbohydrates through receptors.

Yeasts and fungal systems are commonly used to produce recombinant proteins and biopharmaceuticals. Glycoengineered yeasts capable of producing humanized glycoproteins demonstrated tremendous potential and promise as alternatives to mammalian cell cultures (Gerngross et al., 2004). Understanding the glycosylation of yeasts may help to achieve maximum biotechnological potential and to ensure functionality and safety of glycosylated heterologous proteins. This dissertation revealed a number of other promising targets for biotechnology. Considering the industrial applicability of mannosidases, the search for the presence of putative mannosidases was explored since some of the unique novel *N*-linked glycan structures were relatively shorter and contained a maximum of 4 mannose residues (chapters 2 and 3). True enough,

some putative mannosidases were identified as mentioned in chapter 2 and 3 which can be used for future biotechnological work.

On the basis of the structures of the M4- and M6-sized glycans elucidated in this dissertation, it can be presumed that these were results of trimming by possible novel α mannosidases during *N*-linked glycan processing. Certain α1-2/1-3 and/or α1-6 mannosidases could have cleaved the mannose residues resulting in the M4- and M6-sized PA-glycan structures in the three species. Putative GH38 mannosidases were found to be potentially harbored by certain basidiomycetous strains. The GH38 mannosidases may either have dual specifity to α1-3/1-6 or α1-6 mannoses alone, or harbor a broad specific activity againts α1-2/1-3/1-6 mannoses (www.cazy.org). Furthermore (BLAST) analysis revealed the presence of putative mannosidase genes and proteins (annotated as XP_014659398.1, XP_014654165.1, and XP_014658277.1 in NCBI database) within the GH 38, 47 and 92 families, in *P. antarctica* JCM 10317 and T-34. Should these target mannosidases have distinct specificities for α mannoses in distinct positions, then this should ease up the structural analysis of glycans. Furthermore, the availability of commercial enzymes with specific action on α1-3 or α1-6 mannoses will make glycan analysis easier. These should be the targets for future biotechnological work. This glycan information can be useful with regard to biotechnology since these novel target enzymes may be studied for industrial or medical applications, in glycan design and analysis work.

.

The findings in chapter 2 that the combination of citrate buffer extraction and hydrazinolysis glycan release is the best among other tested combinations is a contribution leading

to a more standardized glycan analysis process, at least for the yeasts. With this contribution, succeeding researches on yeast glycans may use the process that this dissertation employed, effectively clarifying the notion that other combinations may be advantageous or disadvantageous. In essence, the streamlining of the glycan process for future work is a welcome addition to glycobiological work process. This clearly showed that a glycobiology-based baseline survey approach can be used to find novel candidate proteins. This can also be juxtaposed to their possible biotechnological prospects for industrial or scientific utilization. In the case of *P. anatarctica* which is currently being used to produce lipids, the elucidation of the structure of its the *N*-linked glycans may serve as initial basis for condisdering the organism as a platform for the production of other biological proteins and not just lipids.

Prospects Biological Significance

This thesis elucidated that the neutral *N*-linked glycan structures of the basidiomycetous yeasts *S. paphiopedili*, *P. antarctica* and *M. furfur* provide an information on the *N*-linked glycans of these yeasts. The analysis of the glycan structure of these known commensals and pathogens may provide initial insights into their roles in adhesion, pathogenicity, and virulence. The use of glycans as target biomarkers has been widely used in different diseases and infections, including cancers (Fuster and Esko, 2005; Lebrilla and Joo Ann, 2012). The discovery of the attachment of putative galactofuranose (Gal*f*) (detected in this thesis as galactose) in the *N*-linked glycans of *M. furfur* may serve as targets for diagnosis or even treatment of fungal infections. Gal*f* residues able

to cause immune response to mammals have been reported in a number of eukaryotes including some pathogenic *Aspergillus* species are therefore regarded as target biomarkers in certain fungal diseases such as aspergillosis, onychomycosis and others (Marino et al., 2017; Tefsen et al., 2012). On the other hand, Gal*f* is not known to be produced by mammals and other higher organisms (Marino et al, 2017). This may show that the Gal*f* can have a diagnostic potential for *M. furfur* infections in mammals, including humans. In juxtaposition, Gal*f* may also serve as a target for the treatment of disease through the therapeutics interventions. These Gal*f* are attached by enzymes called as galactofuranosyl transferases (Gal*f*-transferases) which have been well identified in certain *Aspergillus* species (Chihara et al., 2020; Katafuchi et al., 2017).

The removal of these Gal*f* resulted in the decreased integrity of the cell wall, exposure of the mannan structure, reduced virulence and susceptibility to antifungals (Oka, 2017; Schmalhorst et al., 2018; Arentshorst et al., 2019). Gal*f*-transferases may therefore be used as a target to prevent the attachment of Gal*f* residues in glycans, thus reducing the infectivity and virulence of a pathogen. Inhibition of Gal*f*-transferases by searching for potential inhibitors may be a strategy that can be used similarly in the case involving tuberculosis (Ortiz et al., 2019). On the other hand, Matsunaga et al. (2017 and 2015) showed that recombinant *Streptomyces* sp. β-D-galactofuranosidase (Gal*f*-ase) subsequently expressed in *Escherichia coli*, was able to cleave Gal*f* residues from *Aspergillus* galactomannans. And since humans are devoid of Gal*f*, then this potential medicine may also be considered. Lastly, the detection of high mannose glycans which contains α1-2 mannoses in *M. furfur* in this study suggests its possible role in the recognition on target cells. Dectin-2 recognizes α1-2 mannoses during infection by *M. furfur* (Sparber and LeibundGut-Landmann, 2017). It will

also be interesting to know how these terminal mannoses and galactofuranose residues participate in the infection process, detection of infection and potential treatment.

Knowing the roles that *N*-linked glycans and the enzymes that are related to them is of paramount interest. As have been discussed above, the presence of certain glycosylation genes may have biological roles and may serve as targets for biotechnological and biological potential. The characterization of the genes and the corresponsing enzymes responsible for such high mannose and novel glycan structures found in *S. paphiopedili*, *P. antarctica* and *M. furfur* should be done to fully understand their biology. For example, the applicability of glcan information is evident in the case of the *OCH1* which was found to encode a α1-6 mannosyltransferase responsible for the outer chain mannose elongation in yeasts (Munro, 2001; Nagasu et al., 1992). Consequent study on this gene confirmed that the *S. cerevisiae* deletion mutants had a deficiency in mannose outer chain elongation (Nakayama et al., 1992). Furthermore, the *och1* deletion mutants of some other ascomycetous yeast species, such as *S. cerevisiae*, *S. pombe*, *Pichia pastoris*, *Hansenula polymorpha*, *Kluyveromyces lactis*, *Yarrowia lipolytica*, and an ascomycetous filamentous fungus *Neurospora crassa* demonstrated altered morphological phenotypes, slow growth, and other biological process effects indicating that the outer chain *N*-linked glycans are significant for yeast and fungal cell wall integrity, a primary consideration in host-fungus interactions (Nagasu et al., 1992; Barnay-Verdier et al., 2004; Yoko-o et al., 2001; Choi et al. 2003; Kim et al., 2006; Uccletti et al., 2006; Song et al., 2007; Maddi and Free, 2010). Cell aggregation has been found to be affected by the deletion of *och1* in *C. albicans* (Bates et al., 2006). Moreover, it has been found out that α1-6 Man-containing polysaccharides of some important

fungal pathogens, including *C. albicans*, *Aspergillus fumigatus*, and *C. neoformans*, affect virulence by *och1* deletion (Kotz et al., 2010; Park et al., 2012; Leach and Brown, 2012). Likewise, it will be interesting to know the biological effect of the glycosylation-related genes of the three species studied, as well as the various roles of the novel unique glycan stuctures detected.

All things considered, this dissertation may serve as a point to jumpstart future investigations concerning the roles of the high mannose-type *N*-linked glycans in host-fungus interactions and other biological roles since the most dominant glycans detected for both the commensal and pathogenic ustilaginomycetes were of the high-mannose type. In yeast, protein glycosylation plays key roles in the quality control of secretory proteins, and particularly in maintaining cell wall integrity. Moreover, in pathogenic yeasts, glycans assembled on cell-surface glycoproteins can mediate their interactions with host cells (Masuoka, 2004). Thus, a comprehensive understanding of protein glycosylation in various yeast species and defining glycan structure characteristics can provide useful information for their biotechnological and clinical implications. Yeast-specific glycans are a target for glyco-engineering; implementing human-type glycosylation pathways in yeast can aid the production of recombinant glycoproteins with therapeutic potential. The virulence associated glycans of pathogenic yeasts could be exploited as novel targets for antifungal agents.

Conclusion

In conclusion, the elucidation of the various unique neutral *N*-linked glycans provides us the necessary first step in understanding the glycosylation of *S. paphiopedili*, *P. antarctica* and *M. furfur*. In chapter 2, it is reported that high mannose type *N*-linked glycans were detected in the neutral *N*-linked glycan structures of *P. antarctica* and *M. furfur*. Interestingly, the two yeast species shared the most abundant glycan, M8A, with *S. paphiopedili*, also classified under Ustilaginomycotina (chapter 3) (Flores et al., 2017). Post-translational modifications, such as *N*-linked glycosylation, are considered as very important processing step in preparing functional proteins. This dynamic interplay between elucidated glycan information and biotechnology is exemplified further by the list of novel glycosylation motifs that had been analyzed and the enzymes that had been discovered thereafter. Various applications of glycan studies have been continuously explored. Glycosylation studies entailed the deciphering of the molecular mechanisms of glycosylation and have also paved the way for the production of beneficial proteins. The applicability of glycan studies has not been limited to the production of humanized pharmaceuticals using different hosts.

Meanwhile in chapter 3, the confirmed Man residues of neutral *N*-linked glycans of the three species were reported to range from 3 to 9 residues, which found within the range of *S. paphiopedili* but differ with those found in *Saccharomyces* and *Schizosaccharomyces* carrying hypermannosylated glycans (Gemmille and Trimble, 1999*;* Flores et al., 2017*).* This is probably due to the close phylogenetic relationships among the three basidiomycetous yeast species.

Analysis of the other representative species within the subphylum Ustilaginomycotina and other subphyla will expand the current baseline information which might provide an initial point towards the comprehension of the significance of *N*-linked glycans in biological functions, and possibly, even in evolution. Furthermore, monosaccharide component analysis of the peak corresponding to the hypermannosylated neutral *N*-linked glycans of *M. furfur* (chapter 3) revealed the presence of Gal-PA indicative of the presence of putative galactofuranose residues consistent with previous report. Extensive and intensive analysis of putative mannosidases in ustilaginomyceteous yeasts is a potential jumping point to conduct. This information is necessary for a clearer elucidation of the *N*-linked glycosylation pathway and for possible future utilization of these putative mannosidases for biotechnological applications. The elucidation of the structures of predominant neutral *N*-linked glycans (chapters 2 and 3) opened up an avenue for the appreciation of the vastness of this major post-translational modification. The grandeur of glycosylation designing underscores its importance in a vast gamut of biological processes, some of which are unknown yet to the scientific community. This study was able to create baseline information of *N*-linked glycosylation in the less studied basidiomycetous yeasts. The ustilaginomycetous yeast representatives studied possess simpler neutral *N*-linked glycan structure than those of commonly studied true yeasts belonging to phylum Ascomycota such as *S. cerevisiae*. Consequently, the preponderance and prevalence of smaller-sized glycans raised the question of whether this is a result of a different initial stages of glycosylation or the inactivity of mannosyltransferases in adding mannoses or the activity of mannosidases in trimming the terminal mannoses or the combination of these causes. The view that the initial stages of *N*-glycosylation are conserved for eukaryotic organisms is still a widely accepted concept; therefore, either the inactivity of mannosyltransferases or the activity of mannosidases would have caused the production of smaller sized glycans.

The year 2020 and the world's current battle againsts the coronavirus disease 2019 (COVID-19) pandemic presents an opportunity to draw interest and appreciation to glycan studies not just in the academic and scientific community but with normal people. COVID-19 has undoubtedly caused widespread disease and fear of infection. The race to finding a cure or a vaccine lies on a clear analysis of the pathogenicity and molecular mechanism of the disease (Yang and Wang, 2020). The S protein, a glycoprotein, is regarded as one candidate to become a vaccine to help conquer the COVID-19 pandemic, whether just a certain portion or the whole S protein (Robson, 2020; Zhang et al., 2020). The whole research world is focused on addressing this issue where glycobiology and glycobiotechnology plays an integral role in it. The evolution of the glycosylation machinery and the existence of similarly functioning glycosidases across closely-related species may lead to similarities in the glycan fingerprints. As mentioned in chapter 4, it would be interesting to investigate these glycosylation-related genes to provide a better understanding of Ustilaginomycetes glycosylation. While it would be beneficial to conduct an intensive investigation about the *N*-linked glycan structures of Ustilaginomycotina, the analysis of the putative mannosidases is also necessary. The isolation, characterization, and search for these mannosidases is currently underway. In general, the information established in this study should provide understanding of the *N*-linked glycosylation pathway, which should pave the way for an analysis of related putative mannosidase enzymes with potential biotechnological applications in the future.

LITERATURE CITED

Aebi M, Bernasconi R, Clerc S, Molinari M. 2009. *N*-glycan structures: recognition and processing in the ER. *Trends Biochem Sci* 35: 74−82.

Aime MC, Toome M, McLaughlin DJ. 2014. Pucciniomycotina. In: McLaughlin DJ, Spatafora JW. (eds), The mycota. vol. VII. Part A: systematics and evolution, 2nd ed. Springer-Verlag, Berlin. 271–294.

Agard NJ, Bertozzi CR. 2009. Chemical approaches to perturb, profile, and perceive glycans. *Acc Chem Res* 42: 788–797.

Apweiler R, Hermjakob H, Sharon, N. 1999. On the frequency of protein glycosylation, as deduced from analysis of the SWISS-PROT database. *Biochim Biophys Acta* 1473: 4–8.

Arentshorst M, de Lange D, Park J, Lagendijk E, Alazi E, van Hondel C, Ram A. 2019. Functional analysis of three putative galactofuranosyltransferases with redundant functions in galactofuranosylation in *Aspergillus niger*. *Arch Microbiol* 202: 197–203.

Avis TJ, Cheng YL, Zhao YY, Bolduc S, Neveu B, Anguenot R, Labbe C, Belzile F, Belanger RR. 2005. The potential of *Pseudozyma* yeastlike epiphytes for the production of heterologous recombinant proteins. *Appl Microbiol Biotechnol* 69: 304–311.

Barnay-Verdier S, Boisrame A, Beckerich JM. 2004. Identification and characterization of two α-1,6-mannosyltransferases, anl1p and och1p, in the yeast *Yarrowia lipolytica*. *Microbiology* 150: 2185–2195.

Bartnicki-Garcia S. 1968. Cell wall chemistry, morphogenesis and taxonomy of fungi. *Annu Rev Microbiol* 11: 87–108.

Bartnicki-Garcia, S. 1987. The cell wall in fungal evolution. In A. D. M. Rayner, C. M. Brasier, and D. Moore ed. Evolutionary biology of the fungi. Cambridge University Press, New York, USA. 389–403.

Bates S, Hughes HB, Munro CA. 2006. Outer chain *N*-glycans are required for cell wall integrity and virulence of *Candida albicans. J Biol Chem* 281: 90–98.

Bauer R, Begerow D, Sampaio JP, Weiß M, Oberwinkler F. 2006. The simple-septate basidiomycetes: a synopsis. *Mycol Prog* 5: 41–66.

Bauer R, Begerow D, Oberwinkler F, Piepenbring M, Berbee ML. 2001. Ustilaginomycetes. In: McLaughlin DJ, McLaughlin EJ, Lemke P (eds), The mycota. vol. VIII: Part B. Systematics and evolution. Springer-Verlag, Berlin. 57–84.

Begerow D, Stoll M, Bauer R. 2007. A phylogenetic hypothesisof Ustilaginomycotina based on multiple gene analysesand morphological data. *Mycologia* 98: 906–916.

Berends E, Ohm R, de Jong J, Rouwendal G, Wosten H, Lugones L, Bosh D. 2009. Genomic and biochemical analysis of *N*-glycosylation in the mushroom-forming basidiomycete *Schizophyllum commune. Appl Environ Microbiol* 75: 4648–4652.

Boekhout T. 1987. Systematics of anamorphs of Ustilaginales (smut fungi) – a preliminary survey. *Stud Mycol* 30: 137–149.

Boekhout T. 1995. *Pseudozyma bandoni* emend. Boekhout, agenus for yeast-like anamorphs of ustilaginales. *J Gen Appl Microbiol* 41: 359–366.

Boekhout T, Fell JW. 1998. *Pseudozyma bandoni* emend. Boekhout and a comparison with the yeast state of *Ustilago maydis* (de Candolle) Corda, p 790–797. In: Kurtzman CP, Fell JW. (eds). The yeasts: a taxonomic study, 4th ed. Elsevier Science, Amsterdam, The Netherlands. 790–797.

Boekhout T, Fonseca A, Sampaio JP. 2011. Discussion of teleomorphic and anamorphic basidiomycetous yeasts. In: Kurtzman CP, Fell JW, Boekhout T. (eds). The yeasts: a taxonomic study, 5th ed. Elsevier Science, Amsterdam, The Netherlands. 1339–1372.

Boekhout T. 1991. A revision of ballistoconidia-forming yeasts and fungi. *Stud Mycol* 33: 1–194.

Boratyn GM, Camacho C, Cooper PS, Coulouris G, Fong A, Ma N, Madden T, Matten W,

McGinnis S, Merezhuk Y, Reytselis Y, Sayers E, Tao T, Ye J, Zaretsyaka I. 2013. BLAST: A more efficient report with usability improvements. *Nucleic Acids Res* 41: 29–33.

Burda P, Aebi M. 1999. The dolichol pathway of *N*-linked glycosylation. *Biochim Biophys Acta* 426: 239−257.

Buser R, Lazar Z, Kaser S, Kunzler M, Aebi M. 2010. Identification, characterization, and biosynthesis of a novel *N*-glycan modification in the fruiting body of the basidiomycete *Coprinopsis cinerea. J Biol Chem* 285: 10715–10723.

Chihara Y, Tanaka Y, Izumi M, Hagiwara D, Watanabe A, Takegawa K, Kamei K, Shibata N, Ohta K, Oka T. 2020. Biosynthesis of β-(1,5)-galactofuranosyl chains of fungal-type and *O*-mannose-type galactomannans within the invasive pathogen *Aspergillus fumigatus*. *mSphere* 5: e00770–19.

Choi K, Bobrowicz P, Davidson C, Hamilton R, Kung H, Li H, Miele G, Nett H, Wildt S, Gerngross TU. 2003. Use of combinatorial genetic libraries to humanize *N*-linked glycosylation in the yeast *Pichia pastoris*. *Proc Natl Acad Sci* USA 100: 5022–5027.

Connell LB, Redman R, Rodriguez R, Barrett A, Iszard M, Fonseca A. 2010. *Dioszegia antarctica* sp. nov. and *Dioszegia cryoxerica* sp. nov., psychrophilic basidiomycetous yeasts from polar desert soils in Antarctica. *Int J Syst Evol Microbiol* 60:1466–72.

Cubero B, Nakagawa Y, Jiang X, Miura K, Raghothama K, Bressan R, Hasegawa P, Pardo J. 2009. The phosphate transported PHT46 is a determinant of salt tolerance that is localized to the Golgi apparatus of *Arabidopsis*. *Mol Plant* 3: 535−552.

Dalziel M, Crispin M, Scanlan CN, Zitzmann N, Dwe RA. 2014. Emerging principles for the therapeutic exploitation of glycosylation. *Science* 343: 1235681.

Deshpande N, Wilkins MR, Packer N, Nevalainen H. 2008. Protein glycosylation pathways in filamentous fungi. *Glycobiology* 18: 626–637.

Elling L. 2007. Glycobiotechnology: Enzymes for the synthesis of nucleotide sugars. *Adv Biochem Eng Biotechnol* 58: 89–144.

Feizi T, Fazio F, Chai W, Wong CH. 2003. Carbohydrate microarrays - a new set of technologies at the frontiers of glycomics. *Curr Opin Struct Biol* 13: 637–645.

Flores RJD, Ohashi T, Kawasaki H, Fujiyama K. 2017. The neutral *N*-linked glycans of the ustilaginomycete yeast *Sympodiomycopsis paphiopedili*. *Yeast* 34: 305–307.

Fournier T, Medjoubi N, Porquet D. 2000. Alpha 1-acid glycoprotein. *Biochim Biophys Acta* 1482: 157−171.

Fukuzawa Y, Kagaya K, Shinoda T. 1995. Cell wall polysaccharides in pathogenic yeasts. *Curr Top Med Mycol* 6: 198–219.

Fuster M, Esko JD. 2005. The sweet and sour of cancer: Glycans as novel therapeutic targets. *Nat Rev Cancer* 5: 526–542.

Gemmill TR, Trimble RB. 1999. Overview of *N*- and *O*-linked oligosaccharide structures found in various yeast species. *Biochim Biophys Acta* 1426: 227–237.

Gerngross TU. 2004. Advances in the production of human therapeutic proteins in yeasts and filamentous fungi. *Nat Biotechnol* 22: 1409–1414.

Goldstein IJ, Hollerman CE, Merrick JM. 1965. Protein-carbohydrate interaction. I. The interaction of polysaccharides with concanavalin A. *Biochim Biophys Acta* 97: 68–76.

Golubev VI, Kulakovskaia TV, Kulakovskaia EV, Golubev NV. 2004. The fungicidal activity of an extracellular glycolipid from *Sympodiomycopsis paphiopedili*. *Mikrobiologia* 73:841–845.

Grass J, Pabst M, Kolarich D, Poltl G, Leonard R, Brecker L, Altman F. 2010. Discovery and structural characterization of fucosylated oligomannosidic *N*-glycans in mushrooms. *J Biol Chem* 296: 5987– 5994.

Grobe K, Ledin J, Ringvall M, Holmborn K, Forsberg E, Esko JD, Kjellen L. 2002. Heparan sulfate and development: Differential roles of the *N*-acetylglucosamine *N*-deacetylase/*N*-sulfotransferaseisozymes. *Biochim Biophys Acta* 1573: 209–215.

Gavel Y, von Heijne G. 1990. Sequence differences between glycosylated and non-glycosylated Asn-X-Ths/Ser acceptor sites: implications for protein engineering. *Protein Eng* 3: 433−442.

Guého E, Improvisi L, Christen R, de Hoog GS. 1993. Phylogenetic relationships of *Cryptococcus neoformans* and some related basidiomycetous yeasts determined from partial large subunit rRNA sequences. *Antonie van Leeuwenhoek* 63: 175–189.

Hamid B, Rana BS, Chauhan D, Singh P, Mohiddin FA, Sahay S, Abidi I. 2014. Psychrophilic yeasts and their biotechnological applications- a review. *Afr J Biotechnol* 13: 2188–2197.

Harvey DJ, Merry AH, Royle L, Campbell MP, Dwek RA, Rudd PM. 2009. Proposal for a standard system for drawing structural diagrams of *N*- and *O*-linked carbohydrates and related compounds. *Proteomics* 9: 3796–3801.

Hase S, Ikenaka T, Matsushima Y. 1978. Structure analysis of oligosaccharides by tagging of the reducing end sugars with a fluorescent compound. *Biochem Biophys Res Commun* 85: 57–263.

Hase S, Hatanaka K, Ochiai K, Shimizu H. 1992. Improved method for the component sugar analysis of glycoproteins by pyridylamino sugars purified with immobilized boronic acid. *Biosci Biotechnol Biochim* 56: 1676–1677.

Hamilton SR, Gerngross TU. 2007. Glycosylation engineering in yeast: the advent of fully humanized yeast. *Curr Opin Biotechnol* 5: 387–92.

Harju S, Fedosyuk H, Peterson KR. 2004. Rapid isolation of yeast genomic DNA: Bust n' Grab. *BMC Biotechnol* 4: 8.

Herrmann M, von der Lieth CW, Stehling P, Reutter W, Pawlita M. 1997. Consequences of subtle sialic acid modification on the murine polyomavirus receptor. *J Virol* 71: 5922–5931.

Hibett DS. 2006. A phylogenetic overview of the agaromycotina. *Mycologia* 98: 912–25.

Hibbett DS, Binder M, Bischoff JF, Blackwell M, Cannon PF, Eriksson OE, Huhndorf S, James T, Kirk PM, Lücking R, Lumbsch T, Lutzoni F, Matheny PB, Mclaughlin DJ, Powell MJ, Redhead S, Schoch CL, Spatafora JW, Stalpers JA, Vilgalys R, Aime MC, Aptroot A, Bauer R, Begerow D, Benny GL, Castlebury LA, Crous PW, Dai Y-C, Gams W, Geiser DM, Griffith GW, Gueidan C, Hawksworth DL, Hestmark G, Hosaka K, Humber RA, Hyde K, Ironside JE, Kõljalg U, Kurtzman CP, Larsson K-H, Lichtwardt R, Longcore J, Miądlikowska J, Miller A, Moncalvo JM, Mozley-Standridge S, Oberwinkler F, Parmasto E, Reeb V, Rogers JD, Roux C, Ryvarden L, Sampaio JP, Schüßler A, Sugiyama J, Thorn RG, Tibell L, Untereiner WA,

Walker C, Wang Z, Weir A, Weiß M, White MM, Winka K, Yao Y-J, Zhang N. 2007. A higher-level phylogenetic classification of the fungi. *Mycol Res* 111: 509–547.

Hua M, Chi Z, Liu G, Budzar M. 2010. Production of a novel and cold active killer toxin by *Mrakia frigida* 2E00797 isolated from sea sediment in Antarctica. *Extremophiles* 14: 515–521.

Jung E, Veuthey AL, Gasteiger E, Bairoch A. 2001. Annotation of glycoproteins in the SWISS-PROT database. *Proteomics* 1: 262–268.

Katafuchi Y, Li Q, Tanaka Y, Shinozuka S, Kawamitsu Y, Izumi M, Ekino K, Mizuki K, Takegawa K, Shibata N, Goto M, Nomura Y, Ohta K, Oka T. 2017. GfsA is a β1,5-galactofuranosyltransferase involved in the biosynthesis of the galactofuran side chain of fungal-type galactomannan in *Aspergillus fumigatus*. *Glycobiology* 27: 568–581.

Kiessling LL, Gestwicki JE, Strong LE. 2000. Synthetic multivalent ligands in the exploration of cell-surface interactions. *Curr Opin Chem Biol* 4: 696–703.

Kirk P, Cannon P, Minter D, Stalpers J. 2008. Dictionary of the Fungi, 10th ed. CABI Books, Wallingford, United Kingdom. 211

Kim MW, Kim EJ, Kim JY, Park JS, Oh DB, Shimma Y, Chiba Y, Jigami Y, Rhee SK, Kang HA. 2006. Functional characterization of the *Hansenula polymorpha HOC1*, *OCH1*, and *OCR1*

genes as members of the yeast *OCH1* mannosyltransferase family involved in protein glycosylation. *J Biol Chem* 281: 6261–6272.

Kitamoto D, Haneishi K, Nakahara T, Tabuchi T. 1990. Production of mannsoylerythritol lipids by *Candida antarctica* from vegetable oils. *Agric Biol Chem* 54: 37–40.

Kitamoto D, Isoda H, Nakahara T. 2002. Functional and potential applications of glycolipid biosurfactants. *J Biosci Bioeng* 94: 187–201.

Kitamoto D, Morita T, Fukuoka T, Konishi M. Imura T. 2009. Self-assembling properties of glycolipid biosurfactants and their potential applications. *Curr Opin Colloid Interface Sci* 14: 315–328.

Khoury GA, Baliban RC, Floudas CA. 2011. Proteome-wide post-translational modification statistics: frequency analysis and curation of the swiss-prot database. *Sci Rep* 1: 90.

Kornfeld R, Kornfeld S. 1985. Assembly of asparagine-linked oligosaccharides. *Annu Rev Biochem* 54: 631–64.

Kotsias M, Blanas A, van Vliet SJ, Pirro M, Spencer DR, Kozak R. 2019. Method comparison for *N*-glycan profiling: towards the standardization of glycoanalytical technologies for cell line analysis. *PLoS One* 14: e0223270.

Kotz A, Wagener J, Engel J, Routier FH, Echtenacher B, Jacobsen I, Heesemann J, Ebel F. 2010. Approaching the secrets of *N*-glycosylation in *Aspergillus fumigatus*: characterization of the AfOch1 protein. *PLoS One* 5: e15729.

Kukuruzinska MA, Bergh MLE, Jackson BL. 1987. Protein glycosylation in yeasts. *Annu Rev Biochem* 56: 915–944.

Kukuruzinska MA, Lennon K. 1998. Protein *N*-glycosylation: molecular genetics and functional significance. *Crit Rev Oral Biol Med* 9: 415–448.

Kulakovskaya TV, Shashkov AS, Kulakovskaya EV, Golubev WI. 2004. Characterization of an antifungal glycolipid secreted by the yeast *Sympodiomycopsis paphiopedili*. *FEMS Yeast Res* 5: 247–252.

Latge JP. 2007. The cell wall: carbohydrate armour of the cell. *Molec Microbiol* 66: 279–290.

Leach MD, Brown AJ. 2012. Post-translational modifications of proteins in the pathobiology of medically relevant fungi. *Eukaryot Cell* 11: 98–108.

Lebrilla C, Joo An H. 2012. The prospects of glycan biomarkers for the diagnosis of diseases. *Mol Biosyst* 5: 17–20.

Lewis L, Bain J, Lowes C, Gillespie C, Rudkin F, Gow N, Erwig L. 2012. Stage specific assessment of *Candida albicans* phagocytosis by macrophages identifies cell wall composition and morphogenesis as key determinants. *PLoS Pathog* 8: 1–13.

Lee DK, Bahn YS, Kim HJ, Chung SY, Kang HA. 2014. Unraveling the novel structure and biosynthetic pathway of O-linked glycans in the golgi apparatus of the human pathogenic yeast *Cryptococcus neoformans*. *J Biol Chem* 290: 1861–1863.

Li Y. 1967. Studies on the glycosidases in jack bean meal I. Isolation and properties of α-mannosidase. *J Biol Chem* 242: 5474–5480.

Lombard V, Galaconda Ramulu H, Drula E, Coutinho PM, Henrissat B. 2014. The carbohydrate-active enzymes database (CAZy) in 2013. *Nucleic Acids Res* 42: 490–495.

Looke M, Kristjuhan K, Kristjuhan A. 2011. Extraction of genomic DNA from yeasts for PCR-based applications. *Biotechniques* 50: 325–328.

Maddi A, Free SJ. 2010. α-1,6-Mannosylation of *N*-linked oligosaccharide present on cell wall proteins is required for their incorporation into the cell wall in the filamentous fungus *Neurospora crassa*. *Eukaryot Cell* 9: 1766–1775.

Magalhaes R, Bona de Mondino S, da Silva M, Nishikawa M. 2008. Morphological and biochemical characterization of the etiological agents of white piedra. *Mem Ints Oswaldo Cruz* 103: 786–90.

Matheny PB, Curtis JM, Hofstetter V, Aime MC, Moncalvo J-M, Ge Z-W, Yang Z-L, Slot JC, Ammirati JF, Baroni TJ, Bougher NL, Hughes KW, Lodge DJ, Kerrigan RW, Seidl MT, Aanen DK, DeNitis M, Daniele GM, Desjardin DE, Kropp BR, Norvell LL, Parker A, Vellinga EC, Vilgalys R, Hibbett DS. 2007. Major clades of Agaricales: a multi-locus phylogenetic overview. *Mycologia* 98: 984–997.

Matsunaga E, Higuchi Y, Mori K, Yairo N, Toyota S, Oka T. 2017. Characterization of a PA14 domain-containing galactofuranose-specific β-d-galactofuranosidase from *Streptomyces* sp. *Biochem Mol Biol* 81: 1314–1319.

Matsunaga E, Higuchi Y, Mori K. 2015. Identification and characterization of a novel galactofuranose-specific β-D-galactofuranosidase from *Streptomyces* species. *PLoS One* 10: e0137230.

Maley F, Trimble RB, Tarentino AL, Plummer TH Jr. 1989. Characterization of glycoproteins and their associated oligosaccharides through the use of endoglycosidases. *Anal Biochem* 180: 195–204.

Marino C, Rinflerch A, Lederkremer R. 2017. Galactofuranose antigens, a target for diagnosis of fungal infections in humans. *Future Sci OA* 3: FSO199.

Mariño K, Bones J, Kattla JJ, Rudd PM. 2010. A systematic approach to protein glycosylation analysis: a path through the maze. *Nat Chem Biol* 10:713–23.

Masuoka J, Hazen KC. 2004. Cell wall mannan and cell surface hydrophobicity in *Candida albicans* serotype A and B strains. *Infect Immun* 72: 6230–6236.

Masuoka J. 2004. Surface glycans of *Candida albicans* and other pathogenic fungi: physiological roles, clinical uses and experimental challenges. *Clin Microbiol Rev* 17: 281–310.

McKenzie CGJ, Koser U, Lewis LE, Bain JM, Mora-Montes HM, Barker RN, Gow NAR, Erwig LP. 2010. Contribution of *Candida albicans* cell wall components to recognition by and escape from murine macrophages. *Infect Immun* 4: 1650–1658.

Mitra N, Sharon N, Surolia A. 2003. Role of *N*-linked glycan in the unfolding pathway of *Erythrina corallodendron* lectin. *Biochemistry* 42: 12208–12216.

Mora-Montes H, Bates S, Netea M, Castillo L, Buurman A, Diaz-Jimenez D, Kullberg B, Brown A, Odds F, Gow N. 2010. A multifunctional mannosyltransferase family in *Candida albicans*

determines cell wall mannan structure and host fungus interactions. *J Biol Chem* 284: 12087–12095.

Morita T, Koike H, Koyama Y, Hagiwara H, Ito E, Fukuoka T, Imura T, Machida M, Kitamoto D. 2013. Genome sequence of the basidiomycetous yeast *Pseudozyma antarctica* T-34, a producer of the glycolipid biosurfactants mannosylerythritol lipids. *Genome Announc* 12: e00064–63.

Middelhoven W, Scorzetti G, Fell J. 2004. Systematics of the anamorphic basidiomycetous yeast genus *Trichosporon* Behrend with the description of five novel species. *Int J Syst Evol Micr* 54: 975–986.

Munro S. 2001. What can yeast tell us about *N*-linked glycosylation in the Golgi apparatus? *FEBS Lett* 498: 223–227.

Nagasu T, Shimma Y-I, Nakanishi Y, Kuromitsu J, Iwama K, Nakayama K-I, Suzuki K, Jigami Y. 1992. Isolation of new temperature-sensitive mutants of *Saccharomyces cerevisiae* deficient in mannose outer chain elongation. *Yeast* 8: 353–47.

Nakayama K, Nagasu T, Shimma Y, Kuromitsu J, Jigami Y. 1992. OCH1 encodes a novel membrane-bound mannosyltransferase: outer chain elongation of asparagine-linked oligosaccharides. *EMBO J* 7: 2511–2519.

Ohashi T, Nakakita S, Sumiyoshi W, Takegawa K. 2010. Production of heterologous glycoproteins by a glycosylation-defective *alg3och1* mutant of *Schizosaccharomyces pombe*. *J Biotechnol* 150: 348–356.

Ohtsubo K, Marth JD. 2006. Glycosylation in cellular mechanisms of health and disease. *Cell* 5: 855–67.

Oka T. 2017. Biosynthesis of galactomannans found in filamentous fungi belonging to Pezizomycotina. *Biosci Biotechnol Biochem* 82: 183–191.

Ortiz C, Completo G, Nacario R, Nellas R. 2019. Potential inhibitors of galactofuranosyltransferase 2 (GlfT2): molecular docking, 3D-QSAR, and in silico ADMETox studies. *Sci Rep* 9: 17096.

Pan W, Liao W, Hagen F, Bart T, Weimin S, Jacques F, Teun B. 2011. Meningitis caused by *Filobasidium uniguttulatum*; case report and overview of literature. *Mycoses* 55: 105–99.

Park JN, Lee DJ, Kwon O, Oh DB, Bahn YS, Kang HA. 2012. Unraveling the unique structure and biosynthesis pathway of *N*-linked glycans in the human fungal pathogen *Cryptococcus neoformans* by glycomics analysis. *J Bio Chem* 287: 19501–19515.

Paulson JC, Colley KJ. 1989. Minireview: Glycosyltransferases. *J Biol Chem* 264: 17615–18.

Prillinger H, Laaser G, Dorfler C, Zeigler K. 1991. A contribution to the systematics and evolution of higher fungi: yeast types in the basidiomycetes. Part IV: dacrymyces-type, tremella-type. *Sydowia* 43: 170–218.

Rademacher TW, Parekh RB, Dwek RA. 1998. Glycobiology. *Annu Rev Biochem* 57: 785–838.

Reyes F, Orellana A. 2008. Golgi transporters: opening the gate to cell wall polysaccharide synthesis. *Curr Opin Plant Biol* 11: 244–251.

Robson B. 2020. COVID-19 Coronavirus spike protein analysis for synthetic vaccines, a peptidomimetic antagonist, and therapeutic drugs, and analysis of a proposed achilles' heel conserved region to minimize probability of escape mutations and drug resistance. *Comput Biol Med* 11: 103749.

Saika A, Koike H, Hori T, Fukuoka T, Sato S, Habe H, Kitamoto D, Morita T. 2014. Draft genome sequence of the yeast *Pseudozyma antarctica* type strain JCM 10317, a producer of glycolipid biosurfactants, mannosylerythritol lipids. 2014. *Genome Announc* 5: e00878–14.

Sandin RL, Rogers AL, Patterson RJ, Beneke ES. 1982. Evidence for mannose-mediated adherence of *Candida albicans* to human buccal cells in vitro. *Infect Immun* 35: 79–85.

Schmalhorst P, Krappmann S, Vervecken W. 2008. Contribution of galactofuranose to the virulence of the opportunistic pathogen *Aspergillus fumigatus*. *Eukaryot Cell* 7: 1268–1277.

Schell WA, Lee AG, Aime MC. 2011. A new lineage in Pucciniomycotina: class Tritirachiomycetes, order Tritirachiales, family Tritirachiaceae. *Mycologia 103: 1331–40.*

Schoberer J, Strasser R. 2011. Sub-compartmental organization of golgi-resident *N*-glycan processing enzymes in plants. *Mol Plant* 2: 220–228.

Scorzetti G, Fell JW, Fonseca A, Tallman AS. 2002. Systematics of basidiomycetous yeasts: A comparison of large subunit D1/D2 and internal transcribed spacer rDNA regions. *FEMS Yeast Res* 2: 495–517.

Sheth CC, Hall R, Lewis L, Brown AJ, Odds FC, Erwig L, Gow NAR. 2011. Glycosylation status of the *C. albicans* cell wall affects the efficiency of neutrophil phagocytosis and killing but not cytokine signaling. *Med Mycol* 49: 513–524.

Shibata N, Saitoh T, Tadokoro Y, Okawa Y. 2009. The cell wall galactomannan antigen from *Malassezia furfur* and *Malassezia pachydermatis* contains *β*-1,6-linked linear galactofuranosyl residues and its detection has diagnostic potential. *Microbiology* 155: 3420–3429.

Shibata N, Ichikawa T, Tojo M, Takahashi M, Ito N, Okubo Y, Suzuki S. 1985. Immunochemical study on the mannans of *Candida albicans* NIH A-207, NIH B-792, and J-1012 strains prepared by fractional precipitation with cetyltrimethylammonium bromide. *Arch Biochem Biophys* 243: 338–348.

Shinozaki Y, Morita T, Cao X-H, Yoshida S, Koitabashi M, Watanabe T, Suzuki K, Sameshima-Yamashita Y, Nakajima-Kambe T, Fujii T, Kitamoto HK. 2013. Biodegradable plastic-degrading enzyme from *Pseudozyma antarctica*: cloning, sequencing, and characterization. *Appl Microbiol Biotechnol* 7: 2951–2959.

Shwarz F, Aebi M. 2011. Mechanisms and principles of *N*-linked protein glycosylation. *Curr Opin Struct Biol* 5: 576–82.

Silva GAD, Bernadil TL, Schaker PDC, Menegotto M, Valente P. 2012. Rapid yeast DNA extraction by boiling and freeze-thawing without using chemical reagents and DNA purification. *Braz Arch Biol Technol* 55: 319–327.

Silva D, Duplessis S, Talhinhas P, Azinheira H, Paulo O, Batista D. 2014. Genomic patterns of positive selection at the origin of rust fungi. *PLoS One* 42: 125–165.

Sparber F, LeibundGut-Landmann S. 2017. Host responses to *Malassezia* spp in the mammalian skin. *Front Immunol* 8: 1614.

Song Y, Choi MH, Park JN, Kim MW, Kim EJ, Kang HA, Kim JY. 2007. Engineering of the yeast *Yarrowia lipolytica* for the production of glycoproteins lacking the outer chain mannose residues of *N*-glycans. *Appl Environ Microbiol* 73: 4446–4454.

Snaith SM, Levvy GA. 1968. Purification and properties of α-D-mannosidase from jack-bean meal. *Biochem J* 110: 663–670.

Sugiyama J, Tokuoka K, Suh S, Hirata A, Komagata K. 1991. *Sympodiomycopsis*: a new yeast-like anamorph genus with basidiomycetous nature from orchid nectar. *Antonie Van Leeuwenhoek* 59: 95–108.

Suh S-O, Sugiyama J. 1994. Phylogenetic placement of the basidiomycetous yeasts *Kondoa malvinella* and *Rhodosporidium dacryoidum*, and the anamorphic yeast *Sympodiomycopsis paphiopedili* by means of 18S rRNA gene sequence analysis. *Mycoscience* 35: 367–375.

Suh S-O, Hirata A, Sugiyama J, Komagata K. 1993. Septal ultrastructure of basidiomycetous yeasts and their taxonomic implications with observations on the ultrastructure of *Erythrobasidium hasegawianum* and *Sympodiomycopsis paphiopedili. Mycologia* 85: 30–37.

Suzuki Y. 2005. Sialobiology of influenza: Molecular mechanism of host range variation of influenza viruses. *Biol Pharm Bull* 28: 399–408.

Suzuki M, Fukuzawa Y. 1982. Immunochemical characterization of *Candida albicans* cell wall antigens: Specific determinant of *Candida albicans* serotype A mannan. *Microbiol Immunol* 26: 387–402.

Takashima M, Deak T, Nakase T. 2001. Emendation of *Dioszegia* with redescription of *Dioszegia hungarica* and two new combinations, *Dioszegia aurantiaca* and *Dioszegia croces. J Gen Appl Microbiol* 47: 75–84.

Takashima M, Van BH, An KD, Ohkuma M. 2011. *Dioszegia rishiriensis* sp. nov., a novel yeast species from soil collected on Rishiri Island, Hokkaido, Japan. *Int J Syst Evol Microbiol* 61: 1736–9.

Tefsen B, Ram A, van Die I, Routie F. 2012. Galactofuranose in eukaryotes: aspects of biosynthesis and functional impact. *Glycobiology* 22: 456–459.

Tendersoo L, Sanchez-Ramirez S, Koljalg U, Bahram M, Doring M, Schigel D, May T, Ryberg M, Abarenkov K. 2018. High-level classification of the Fungi and a tool for evolutionary ecological analyses. *Fungal Divers* 90: 135−159.

Trimble RB, Tarentino AL. 1991. Identification of distinct endoglycosidase (endo) activities in *Flavobacterium meningosepticum:* endo F1, endo F2 and endo F3. *J Biol Chem 266*: 1646–1651.

Trochine A, Turchetti B, Vaz ABM, Brandao L, Rosa LH, Buzzini P, Rosa C, Libkind D. 2017. Description of *Dioszegia patagonica* sp. nov., a novel carotenogenic yeast isolated from environments. *Int J Syst Evol Microbiol* 11: 4332–4339.

Uccelletti D, Farina F, Rufini S, Magnelli P, Abeijon C, Palleschi C. 2006. The *Kluyveromyces lactis* α1,6-mannosyltransferase KlOch1p is required for cell wall organization and proper functioning of the secretory pathway. *FEMS Yeast Res* 6: 449–457.

Upreti RK, Kumar M, Shankar V. 2003. Bacterial glycoproteins: Functions, biosynthesis and applications. *Proteomics* 3: 363–379.

Wang P, Wang H, Gai J, Tian X, Zhang X, Lu Y, Jian Y. 2017. Evolution of protein *N*-glycosylation process in Golgi apparatus which shapes diversity of protein *N*-glycan structures in plants, animals and fungi. *Sci Rep* 7: 40301.

Weiß M, Selosse M-A, Rexer K-H, Urban A, Oberwinkler O. 2004. Sebacinales: a hitherto overlooked cosm of heterobasidiomyceteswith a broad mycorrhizal potential. *Mycol Res* 108: 1003–1010.

Wong-Madden ST, Landry D. 1995. Purification and characterization of novel glycosidases from the bacterial genus *Xanthomonas*. *Glycobiology* 5: 19–28.

Yang P, Wang X. 2020. COVID-19: a new challenge for human beings. *Cellular and Molecular Immunology* 17: 555–557.

Yamada Y, Banno I. 1984. *Fellomyces,* a new anamorphic yeast genus for the Q10-equipped organisms whose conidium is freed by an end-break in the sterigma. *J Gen Appl Microbiol* 30: 523–525.

Yamada Y, Komagata K. 1987. *Mrakia* gen novo. A heterobasidiomycetous yeast genus for the Q8-equipped self-sporulating organisms which produces a unicellular metabasidium, formerly classified in the genus *Leucosporidium*. *J Gen Appl Microbiol* 33: 455–457.

Yoko-o T, Tsukahara K, Watanabe T, Hata-Sugi N, Yoshimatsu K, Nagasu T, Jigami Y. 2001 *Schizosaccharomyces pombe* och1^{+} encodes α1,6-mannosyltransferase that is involved in outer chain elongation of *N*-linked oligosaccharides. *FEBS Lett* 489: 75–80.

Yoshizawa Z, Sato T, Schmid K. 1966. Hydrazinolysis of alpha-1-acid glycoprotein. *Biochim Biophyy Acta* 121: 417–420.

Watanabe T, Morita T, Koike H, Yarimizu T, Shinozaki Y, Sameshima-YamashitaY, Yoshida S, Koitabashi M, Kitamoto H. 2016. High-level recombinant protein production by the

basidiomycetous yeast *Pseudozyma antarctica* under a xylose-inducible xylanase promoter. *Appl Microbiol Biotechnol* 7: 3207–17.

Welti M. 2012. Regulation of dolichol-linked glycosylation. *Glycoconj J* 30: 51–56.

White TJ, Bruns TD, Lee S, Taylor JW. 1990. Amplification and direct sequencing of fungal ribosomal RNA genes for phylogenetics. In: Innis MA, Gelfand DH, Sninsky J, White TJ (eds), PCR protocols: a guide to methods and applications. Academic Press, San Diego. 315–322.

Xu C, Ng DTW. 2015. Glycosylation-directed quality control of protein folding. *Nat Rev Mol Cel Biol* 12: 742–52.

Zhang J, Zeng H, Gu J, Li H, Zheng L, Zou Q. 2020. Progress and prospects on vaccine development againsts SARS-Cov-2. *Vaccines* 8: 153–165.

Ziegler FD, Gemmill TR, Trimble RB. 1994. Glycoprotein synthesis in yeast. Early events in *N*-linked oligosaccharide processing in *Schizosaccharomyces pombe. J Biol Chem* 269: 12527–12535.

LIST OF PUBLICATIONS

Flores RJD, Ohashi T, Kawasaki H, Fujiyama K. 2017. The neutral *N*-linked glycans of the ustilaginomycete yeast *Sympodiomycopsis paphiopedili*. *Yeast* 34: 305–307.

Flores RJD, Ohashi T, Sakai K, Gonoi T, Kawasaki H, Fujiyama K. 2019. The neutral *N*-linked glycans of the basidiomycetous yeasts *Pseudozyma antarctica* and *Malassezia furfur* (subphylum ustilaginomycotina). *J Gen Appl Microbiol* 65: 53–63.

LIST OF CONFERENCES

2015 Society of Biotechnology Japan Annual Meeting. Structural Analysis of the *N*-linked Glycans of Yeasts Belonging to Subphylum Agaricomycotina. (Poster Session) October 2015. Kagoshima Kanko Hotel, Kagoshima, Japan.

41st Annual Convention of the Philippine Society for Biochemistry and Molecular Biology. The *N*-linked glycans of selected basidiomycetous yeasts. (Poster Session). December 2014. Marco Polo Hotel, Cebu City, Philippines.

2014 Meeting of the Japan Society for Carbohydrate Research. Structural Analysis of the *N*-linked glycans of Agaricomycotina Yeasts. (Poster Session). August 2014. Nagoya University, Nagoya, Japan

2014 Meeting of the Japan Society for Bioscience, Biotechnology and Agrochemistry. Structural Analysis of the *N*-linked Glycans of Selected Yeasts Belonging to Subphylum Agaricomycotina. (Oral Session). March 2014. Meiji University, Kanagawa, Japan

2013 Meeting of the Japan Society for Carbohydrate Research. Structural Analysis of the *N*-linked glycans of Basidiomycetous Yeasts. (Poster Session). August 2013. Osaka City University, Osaka, Japan

2013 Meeting of the Japan Society for Bioscience, Biotechnology and Agrochemistry. Structural Analysis of the *N*-linked Glycans of Selected Yeasts Belonging to Subphylum Ustilaginomycotina. (Oral Session) April 2013. Tohoku University, Sendai, Japan

SPECIAL AWARD

Best Presentation Award for Second Year Student in the Master`s Course of the International Program. Structural Analysis of the *N*-glycans of Basidiomycetous Yeasts for Insights on Yeast Taxonomy. December, 2013. Department of Biotechnology. Graduate School of Engineering, Osaka University, Japan.

ACKNOWLEDGEMENT

I dedicate this degree to my Father, Nilo, my mother, Rina and my brother, Roy. I would like to thank God for guiding me all the way from the beginning until the end of this journey and for making all things, good or not-so-good, possible. I would like to extend my deepest gratitude to the people of Japan, MEXT, and Osaka University for providing a beautiful place and an awesome environment and support for doing such valuable research all throughout my stay. I would like to thank my professor Prof. Dr. Kazuhito Fujiyama for all the guidance that he had extended to me and to all the members of the Laboratory of Applied Microbiology of the International Center for Biotechnology, Graduate School of Engineering, Osaka University. I would also like to thank Assistant Prof. Takao Ohashi for all the things he had taught me and for guiding me through these tasks. I also thank Dr. Hiroko Kawasaki for all the guidance and providing the yeasts for the project. I am extending my utmost gratitude to all the members of Fujiyama Lab, Associate Prof. Ryo Misaki, staff of the International Center for Biotechnology and to all collaborators. Also, this would not have been possible without the constant support of my family and friends. Most of all to Prof. Nirianne Palacpac and Tito Noel Palacpac for being a voice of encouragement during trying times. To Ate Marian, Ate Anilyn and Kuya Walter, thank you for always having my back. To all my colleagues back at the Institute of Biological Sciences, in the University of the Philippines Los Baños, thank you. And to my wonderful housemates who I have shared all my frustrations and aspirations which in doing so had led me to where I am now, Ronald, Ivy, Johnry, Kris, Maurice, Jon and Marc, Thank you. And lastly and most importantly to my mother, father and brother, you are all the reason for which I do everything that I do. Thank you all. Thank you, Universe.